AUGMENTATION OF TWO IDENTIFICATION METHODS FOR BATS

By

SHANE SEHEULT, BSc

A Thesis Submitted in Partial Fulfillment of the Requirements for the

Degree of Masters of Science

in the Department of Psychology, Neuroscience & Behaviour

Faculty of Science

Marking Methods for Bat Research

McMaster University MASTERS OF SCIENCE (2023) Hamilton, Ontario

Department of Psychology, Neuroscience & Behaviour

TITLE: Augmentation of two identification methods for bats

AUTHOR: Shane Seheult, B.Sc.

SUPERVISOR: Dr. Paul A. Faure

NUMBER OF PAGES: xi, 101

Acknowledgments

Thank you to my supervisor, Dr. Paul A. Faure, for introducing me into the Bat Lab, guiding me through both my undergraduate and graduate theses, and creating a pleasant lab environment that encourages both curiosity and discovery. I look forward to continuing a PhD in your lab under your supervision.

I would like to thank my Supervisory committee, Dr. Patrick Bennett, Dr. Ian Bruce, and Dr. Reuven Dukas for their guidance throughout my MSc career. I would also like to thank Dr. Alex Borisenko from the University of Guelph for providing the Bat Lab with the p-Chip technology, and for training me on how to use the p-Chip technology. In addition, my work would not be possible without the help of Dawn Graham, Kathleen Delaney, and the staff of the Central Animal Facility who provide exceptional animal care. I would like to thank Raj Panchal for assisting with p-Chip data collection and Joshua Cherney for his assistance with photo collection and analysis of the collagen-elastin patterns. Both Raj and Josh were integral in the completion of this thesis and are remarkable colleagues and friends. I would also like to thank Dr. Lucas Greville for his continued mentorship and guidance during my undergraduate and graduate career.

Thank you to my family: Christian Seheult, Risa Meltzer, Jesse Seheult, Marli Seheult, and Harriet Seheult. They encourage me to work hard and always show their unconditional love and support. Lastly, I would like to thank Sara Scampoli for assisting me in everything I aspire to do. Sara is a true inspiration to me, my strongest support system, and a prominent motivator in my day-to-day life. She truly is the love of my life.

Table of Contents

List of Figures

List of Tables

Declaration on Academic Achievement

Chapter 1 – Introduction

Author: Shane Seheult

Chapter 2 - Scanning efficacy of p-Chips implanted in the wing and leg of the big brown bat (*Eptesicus fuscus*)

Authors: Shane D. I. Seheult, Raj Panchal, Alex V. Borisenko, Patrick J. Bennett, and Paul A. Faure

Publication: Journal of Mammalogy. ID: JMAMM-2023-058.R2.

Comments: S.D.I.S. and R.P. performed experiments; S.D.I.S., P.J.B., and P.A.F. analyzed data; S.D.I.S., A.V.B., P.J.B., and P.A.F. interpreted results of experiments; S.D.I.S. and P.A.F. prepared figures; S.D.I.S., A.V.B., P.J.B., and P.A.F. drafted, edited, and revised manuscript; A.V.B. conceived and designed research.

Chapter 3 - Using HotSpotter to identify individual big brown bats (*Eptesicus fuscus*) via collagen-elastin bundle patterns

Authors: Shane D. I. Seheult, Joshua R. M. Cherney, Paul A. Faure

Publication: In preparation

Comments: J.R.M.C. performed experiments; S.D.I.S. and P.A.F analyzed data; S.D.I.S and P.A.F. interpreted results of the experiments; S.D.I.S. and P.A.F prepared figures; S.D.I.S. and P.A.F. drafted manuscript; S.D.I.S and P.A.F. drafted, edited, and revised manuscript; S.D.I.S conceived and designed research.

Chapter 4 – Conclusion

Author: Shane Seheult

Abstract

All marking methods for identifying bats (order Chiropteran) have practical limitations, with no one method being superior to others. To address these limitations, we proposed and tested the use of two prospective identification methods —p-Chip microtransponder tags and the use of collagen-elastin (CE) bundle patterns as a biomarker— in a captive colony of big brown bats (*Eptesicus fuscus*). For p-Chips, we assessed (1) animal handling time, (2) scan time, (3) number of wand flashes, (4) p-Chip visibility, (5) readability, and (6) the bat's overall condition for two locations: all bats had p-Chips implanted in the wing (n = 30) and some of these bats also had p-Chips implanted in their leg (n = 13). For both locations, average scan times increased over time whereas the number of wand flashes decreased, suggesting p-Chip recording efficacy improves with user experience. The visibility and readability of p-Chips was consistently better for tags injected in the wing compared the leg, emphasizing the wing as the preferred implantation site. A second proposed identification method extends upon the use of manual, visual inspection (Amelon et al. 2017) to examine whether pattern-recognition software can accurately detect and identify individual bats using the pattern of collagen and elastin bundles in the wing. We tested the effectiveness of HotSpotter© to identify adult (n = 24 bats; n = 192 photos) and juvenile (n = 34 pups; n = 136 photos) *E. fuscus* by comparing photos of the wing membrane illuminated by ultraviolet light. We then assessed similarity scores between adults and juveniles separately and quantified the occurrence of correct and incorrect matches. For images of adult bats, 60% of comparisons resulted in a correctly

matched top-ranked image (i.e. an image of the same bat was most similar), whereas 27% of comparisons had a correct top-ranked image for wing membrane photos of juvenile bats. The success rate of obtaining a correct match could be increased by including a larger subset of top-ranked images when selecting possible correct matches. Altogether, these results suggest that p-Chip tags and potentially the use of HotSpotter pattern recognition software are suitable methods for identifying captive *E. fuscus* and may be viable for use in the field and in other bat species.

Chapter 1 – Introduction

Introduction

Techniques used to mark animals for individual identification are critical for ecological studies, to ensure viable data collection. Marking methods typically involve applying some form of mark or tag that is easily identified and distinguishable between tagged individuals. There are various marking methods that are used in both field work and laboratory studies and in a variety of different animals. For bats, researchers have implemented various marking methods to directly alter the bats appearance including punch-marking (Bonaccorso & Smythe, 1972; Bonaccorso et al. 1976; Griffin, 1934), toe-clipping (Stebbings 1978; Kunz & Weise, 2009), hair trimming (Kunz & Weise, 2009, Stebbings, 2004), fur staining (Brack & Twente, 2011; Leblanc et al. 2002; Brooke, 1987; Mohr, 1934), freeze-branding (Lazarus & Rowe, 1975; Sherwin et al. 2002), or apply an external tag such as body piercings (Barnard & Abram, 2004), ear tags (Mohr, 1934), chemiluminescent tags (Punt 1957; Silvy et al. 2012; Barbour & Davis, 1969; Gifford & Griffin, 1960; Buchlear, 1976; LaVal et al. 1977; Hovorka et al. 1996; Britzke et al. 2014), bead necklaces (Barclay & Bell, 1988; Gannon, 1993; Handley et al. 1991), or radio telemetry tags (LeMunyan et al. 1959). See Kunz & Weise (2009) for a review of bat marking methods.

Despite notions of successful use in the wide variety of marking methods used in bat research, there has yet to be a method that is viable for every situation, bat species, and experimental design. Researchers must consider the advantages and disadvantages of the various mark methods when formulating experiments as

one particular method may not suit the needs of the experimental design. For example, applying an external tag may influence the animals behaviour. Some marking methods may require animal handling to apply and record the mark. The need for repeated animal handling may cause stress (Happold & Happold 1997), require that users receive proper animal handling training, and limit the use of the method to periods outside of hibernation (Barclay & Bell, 1988).

Tag visibility is important to help distinguish marked from unmarked animals; however, some marking methods may be virtually invisible (e.g. passive integrative transponder tags are applied under the skin), subject to translocating after being applied (e.g., Barnard 1989), or take time to become visible (e.g. freeze-branding can take up to 2 months to become visible) (Sherwin et al. 2002). The permanence of the marking method is also an important consideration. Marking methods are often classified into short-term (e.g. wing membrane tattoos only last for a few months) (Bonaccorso et al. 1976) or long-term (e.g. banding). Tag permanence may vary across seasons (e.g. molting of bats hair affects hair trimming patterns) (Stebbings, 2004), or completely disappear if tags become unattached from the animal (e.g. Buchlear, 1976).

Tag efficacy is also species dependant as different species have varying tolerance to certain marking methods (e.g. Tidemann, 2002). For instance, Bradbury (1977) attempted to use various marking methods on one of the largest bat species, hammer-headed bat (*Hyspignathus monstrousus*), including bleaching, different types/sizes of forearm bands, reflective tapes and necklaces. The authors found that radiotransmitters were a viable marker for *H. monstrousus*;

however, the added weight of the radiotransmitter reduced their maneuverability during flight (Bradbury, 1977). It has been proposed that flight maneuverability is inversely proportional to increase in mass, such that a 5% increase in added mass would result in a 5% decrease in flight maneuverability and increase the muscle power needed to maintain flight (Caccamise & Heddin, 1985; Aldridge & Brigham, 1988). Conversely, pregnant female bats can fly with up to a 30% increase in body mass without any impacts on foraging success, suggesting a 30% increase in mass may be the upper limit when there is an abundance of food (Aldridge & Brigham, 1988). Therefore, the weight of the external tag must also be considered when selecting a marking method for a specific bat species. Certain tags can be modified to suit specific bat species. For example, it is important when banding animals to use the correct material (e.g. metallic or plastic split rings) (Kunz, 1996), band type (e.g. lipped bands, traditional bird bands) (Hitchcock, 1957), band size, and band placement (e.g. forearm or tibia) (Trapido & Crowe, 1946) to avoid band-related injuries (Phillips, 1985; Baker al., 2001; Herried et al. 1960; Pierson & Fellers, 1994).

Many marking methods have been reported to affect survivability and/or cause injury to the animal. For instance, toe clipping has been discontinued as a marking method as bats rely on their claws for roosting, crawling, and grooming behaviours (Kunz & Weise, 2009; Silvy et al. 2012). Similarly, trimming bats hair may affect their ability to thermoregulate during periods of torpor (Barclay & Bell, 1988; Speakman et al. 2003). For external tags, bats may undergo self-mutilation via chewing, causing the tags to become unreadable (Bonaccorso and

Smythe 1972; Humphrey & Kunz, 1976; Baker et al. 2001). External tags may attract predators (Silvy et al. 2012) or deter prey (Norman et al. 1999) and affect foraging success.

Currently, there is no marking method that is superior to all others or considered perfect. Therefore, it is crucial to expand on possible marking techniques in attempt to reduce the disadvantages and emphasize the advantages associated with marking animals for individual identification. In summary, the ideal marking method should: (1) be easily visible, (2) be relatively permanent, (3) be relatively easy to record, (4) be relatively easy to distinguish marked vs. unmarked individuals, (5) reduce animal handling / stress, (6) reduce injury, (7) work in all (or most) situations (i.e. field-work and laboratory work), (8) be easily distinguishable, (9) work for all (or most) species, and (10) not directly affect animal behaviour.

Chapter 2 – Scanning efficacy of p-Chips implanted in the wing and leg of the big brown bat (*Eptesicus fuscus*)

Abstract

Individual marking techniques are critical for studying animals, especially in the wild. Current marking methods for bats (Order Chiroptera) have practical limitations and some can cause morbidity. We tested the p-Chip (p-Chip Corp.)—a miniaturized, laser light-activated micro-transponder—as a prospective marking technique in a captive research colony of big brown bats (*Eptesicus fuscus*). We assessed long-term readability and post-implantation effects of p-Chips injected subcutaneously above the second metacarpal (wing; n = 30) and the tibia (leg; n = 13 in both locations). Following implantation (day 0), p-Chips were scanned with a hand-held ID reader (wand) on post-implantation days (PIDs) 1, 8, 15, 22, 32, 60, 74, 81, 88, 95, and over one year later (PID 464). For each trial, we recorded: (1) animal handling time, (2) scan time, (3) number of wand flashes, (4) p-Chip visibility, and (5) the bat's overall condition. Average scan times for p-Chips implanted in both the wing and leg increased over the duration of the study; however, the number of wand flashes decreased, suggesting that efficacy of p-Chip recording increased with user experience. Importantly, over 464 days both the visibility and readability of p-Chips in the wing remained high and superior to tags in the leg, establishing the second metacarpal as the preferred implantation site. Observed morbidity and mortality in captive bats with p-Chips was similar to baseline values for bats without these tags. Because scan efficiency on PID 464 was comparable with earlier days, this indicates p-Chips implanted in the wing

may be suitable as a long-term marking method. Our provisional results suggest p-Chips are viable for extended field testing to see if they are suitable as an effective alternative to traditional methods to mark bats.

Resumen

Las técnicas de marcaje individual son fundamentales para el estudio de los animales, especialmente en la naturaleza. Los métodos actuales de marcaje de murciélagos (Chiroptera) tienen limitaciones prácticas y algunos pueden causar morbilidad. Probamos el p-Chip (p-Chip Corp.)—un microtranspondedor miniaturizado activado por luz láser—como técnica de marcaje prospectivo en una colonia en cautiva de murciélagos morenos (*Eptesicus fuscus*). Se evaluó la legibilidad a largo plazo y los efectos post-implantación de los p-Chips inyectados subcutáneamente sobre el segundo metacarpiano (ala; n = 30) y la tibia (pata; n = 13 en ambas localizaciones). Tras la implantación (día 0), se escanearon los p-Chips con un lector de identificación manual (varita) en los días posteriores a la inyección (PID) 1, 8, 15, 22, 32, 60, 74, 81, 88, 95, y más de un año después (PID 464). En cada ensayo se registró: (1) el tiempo total de manipulación del animal, (2) el tiempo de exploración, (3) el número de destellos de proximidad de la varita, (4) la visibilidad del p-Chip, y (5) el estado general del murciélago. Los promedios del tiempo de escaneado de los p-Chips implantados tanto en el ala como en la pata aumentaron a lo largo del estudio; sin embargo, el número de destellos de la varita disminuyó, lo que sugiere que la eficacia del registro del p-Chip aumentó con la experiencia del usuario. A lo largo de 464 días, tanto la visibilidad como la legibilidad de los p-Chips en el ala siguieron siendo altas y superiores a las de las etiquetas en la pata, lo que estableció el segundo metacarpiano como el lugar preferido de implantación. La morbilidad y mortalidad observadas en murciélagos cautivos con p-Chips fue similar a los

valores de referencia de los murciélagos sin estas marcas. Dado que la eficacia del escaneado en el PID 464 fue comparable a la de días anteriores, es probable que los p-Chips implantados en el ala sean adecuados como método de marcado a largo plazo. Nuestros resultados provisionales sugieren que los p-Chips son viables para pruebas de campo prolongadas como alternativa prospectiva a los métodos tradicionales de marcaje de murciélagos.

Introduction

Animal identification with individual marking techniques is important for addressing many questions about wildlife biology. The efficacy of a marking technique depends on the likelihood of follow up encounters with tagged individuals, the permanence of the mark, the ease of mark recognition, and minimization of its impact on animal health, wellbeing, and behaviour (Buchler 1976; Kunz and Weise 2009; Silvy et al. 2012). Thus, animal marking involves balancing performance criteria with ethical considerations (Powell and Proulx 2003). Among mammals, bats (Order Chiroptera) have been a popular subject for mark-recapture studies, leading to important insights into their homing abilities (Mohr 1934; Trapido and Crowe 1946; Cockrum 1956; Dwyer 1966; O'Donnell 2001; Fleming and Eby 2003; Gibbons and Andrews 2004; Campbell et al. 2006; Chaveri et al. 2007; Goldshtein et al. 2021), population dynamics (Dwyer 1969; Humphrey 1971), growth rate (Gibbons and Andrews 2004), survivorship (Hoyle et al. 2001; Leigh and Handley 1991; Young 2001; O'Donnell 2002), development (Kunz and Stern 1995; Kunz and Hood 2000), and behaviour (Dwyer 1970; Bradbury 1977; McCracken and Wilkinson 2000; Reeder et al. 2006; Zubaid et al. 2006).

Many techniques have been developed for marking bats in the field and laboratory (Kunz and Weise, 2009); however, the applicability and impact of a particular technique may differ between species and even individuals, often depending on the ecological and life history context (Bonaccorso et al. 1976; Kunz and Weise 2009; Silvy et al. 2012). Forearm bands are the most widely and

continuously used bat marking technique (Trapido and Crowe 1946; Hitchcock 1965; Greenhall and Paradiso 1968; Stebbings 1978; Phillips 1985). Due to its early adoption, relatively low cost, and ease of application, banding has resulted in the largest and most comprehensive global datasets on bat longevity and movements compared to other marking techniques. Banding efficacy and impact on bat health depend on the species, situation, and type of band (Bonaccorso et al. 1976; Vardon and Tidemann 2002). In some cases, bands may cause injury, decrease foraging success, and increase morbidity and mortality (Herried and Davis 1960; Perry and Beckett 1966; Rybar 1973; Pierson and Fellers 1994; Norman et al. 1999; Baker et al. 2001; O'Shea et al. 2004; Dietz et al. 2006). Such adverse effects have inspired a continued search for alternative marking approaches.

Radio-frequency identification (RFID) markers, specifically passive integrated transponder (PIT) tags, are commonly used to mark bats (Barnard 1989; Want 2006; Voulodimos et al. 2010). Subcutaneous PIT tags are implanted via needle injection, typically along the back between the shoulder blades (Barnard 1989; Rigby et al. 2012). Each PIT tag transmits a unique radio frequency serial identification (ID) number when its solenoid antenna receives radio wave energy from an associated reader (Want 2006). The use of PIT tags also has trade-offs (Barclay and Bell 1988; Rigby et al. 2012). The PIT tag injection may stress the animal because it is invasive (and potentially dangerous) and requires a large (e.g. 12-gauge) needle. Injected PIT tags are not visible to the naked eye but can be felt by palpating the injection site, further increasing animal

handling. PIT tags can also move under the skin after implantation (Barnard 1989) and possibly be expelled from the body through the implantation site (Kunz and Weise 2009). Several studies in bats have examined the impact of PIT tags on recapture rates, body mass, body condition and reproductive success, and found no differences between tagged and untagged animals (Murray and Fuller 2000; Neubaum et al. 2005; Rigby et al. 2012). The placement of PIT tag reader arrays in cave entrances has been shown to have minimal impacts on bat flight and behaviour (Britzke et al. 2014).

More recently, a new marking method has been developed using the p-Chip (p-Chip Corp., Chicago, IL, USA; https://p-chip.com). The p-Chip is a flat square 500 × 500 µm micro-transponder semiconductor tag (mass ~85 µg) activated by red laser light emitted by a compatible hand-held ID reader wand connected to a computer via a universal serial bus (USB) cable. The wand continuously emits lower-power laser light when it is idle; however, as the beam approaches and illuminates the photosensitive cells on the top surface of the p-Chip, the laser operates in higher-power pulsed burst mode and the beam flashes (i.e. flickers) in intensity (Gruda et al. 2010; PharmaSeq, undated white paper). When activated, the p-Chip transmits a unique 9-digit serial ID number as a radio signal that is detected by the wand's sensor. This ID number is then transmitted to the computer and recorded by p-Chip Reader software. The ID readout is nearly instantaneous (<0.01 s).

For a successful read, the p-Chip must be in close proximity to the wand's light-emitting tip and have its photocells facing the wand, with no opaque

materials in between. For this reason, p-Chips are often surface mounted on objects (Jolley-Rogers et al. 2012, Mandecki et al. 2017) or animals (Robinson et al. 2009; Robinson and Mandecki 2011; Tenczar et al. 2014; Mandecki et al. 2016; Hamilton et al. 2019). When used subcutaneously, p-Chips are injected in areas where the skin is thin, translucent, and hairless (Gruda et al. 2010; Chen et al. 2013; Delcourt et al. 2018). Due to their polymer coating, p-Chips are resilient to chemicals, high temperatures, repeated freezing/thawing, and placement in liquid nitrogen (p-Chip Corp., 2020). Therefore, once implanted, p-Chips are expected to function indefinitely.

To date, the p-Chip technology has been successfully adopted for tagging honeybees (Tenczar et al. 2014), ants (Robinson et al. 2009, 2014), and fish (Chen et al. 2013; Delcourt et al. 2018; Faggion et al. 2020; Moore and Brewer, 2021). Among mammals, the only published protocol is for laboratory mice with transponders implanted subcutaneously in the pinna or near the base of the tail, with the latter identified as the preferred location (Gruda et al. 2010). A conference abstract reports using p-Chips to mark bats in the field, but without details of the implantation technique or tag placement (Ngamprasertwong et al. 2022). Our goal was to evaluate the p-Chip as a prospective method to mark bats. We did this by testing the hypothesis that there was no difference in scanning efficiency over time for p-Chips implanted subcutaneously in two anatomical locations—the second metacarpal (i.e., the wing) and the tibia (i.e., the leg)—using a captive research colony of big brown bats (*Eptesicus fuscus*).

Methods & Materials

Animals.—Thirty big brown bats (*Eptesicus fuscus*) were used in this study. All bats were either wild caught as adults in southern Ontario (n = 9) or direct descendants born in captivity (n = 21). Bats were housed in a husbandry facility at McMaster University where the temperature and light varied seasonally following ambient conditions (Skrinyer et al. 2014). The facility consisted of two indoor enclosures (2.5 × 1.5 × 2.3 m; l × w × h), one of which was connected through a hole in the wall to a larger outdoor flight area (2.5 × 3.8 × 2.7 m) that bats could freely access. Food (mealworms; *Tenebrio molitor*) and water were provided *ad libitum*. For the bats we studied (n = 30), the mean ± standard deviation (*SD*) mass was 18.7 ± 4.2 g (range: 11.6 – 30.8 g) and forearm length was 45.25 ± 1.64 mm (range: 40.50 – 47.95 mm). Each bat was individually identified with a colored, numbered, plastic split-ring forearm band and a PIT tag injected subcutaneously between the shoulder blades. Bats were monitored for health changes throughout the study. All experimental procedures were approved by the Animal Research Ethics Board of McMaster University and conformed to the *Guide to the Care and Use of Experimental Animals* published by the Canadian Council of Animal Care and the ASM guidelines for research on live animals (Sikes et al. 2016).

Tag Implantation.—p-Chips were injected subcutaneously in hand-restrained bats by the same operator (AB) on 11 November 2019, using pre-loaded, sterile, flat-tipped 21-gauge needles with plunger purchased from p-Chip Corp., in two predefined locations (Fig. 2.1):

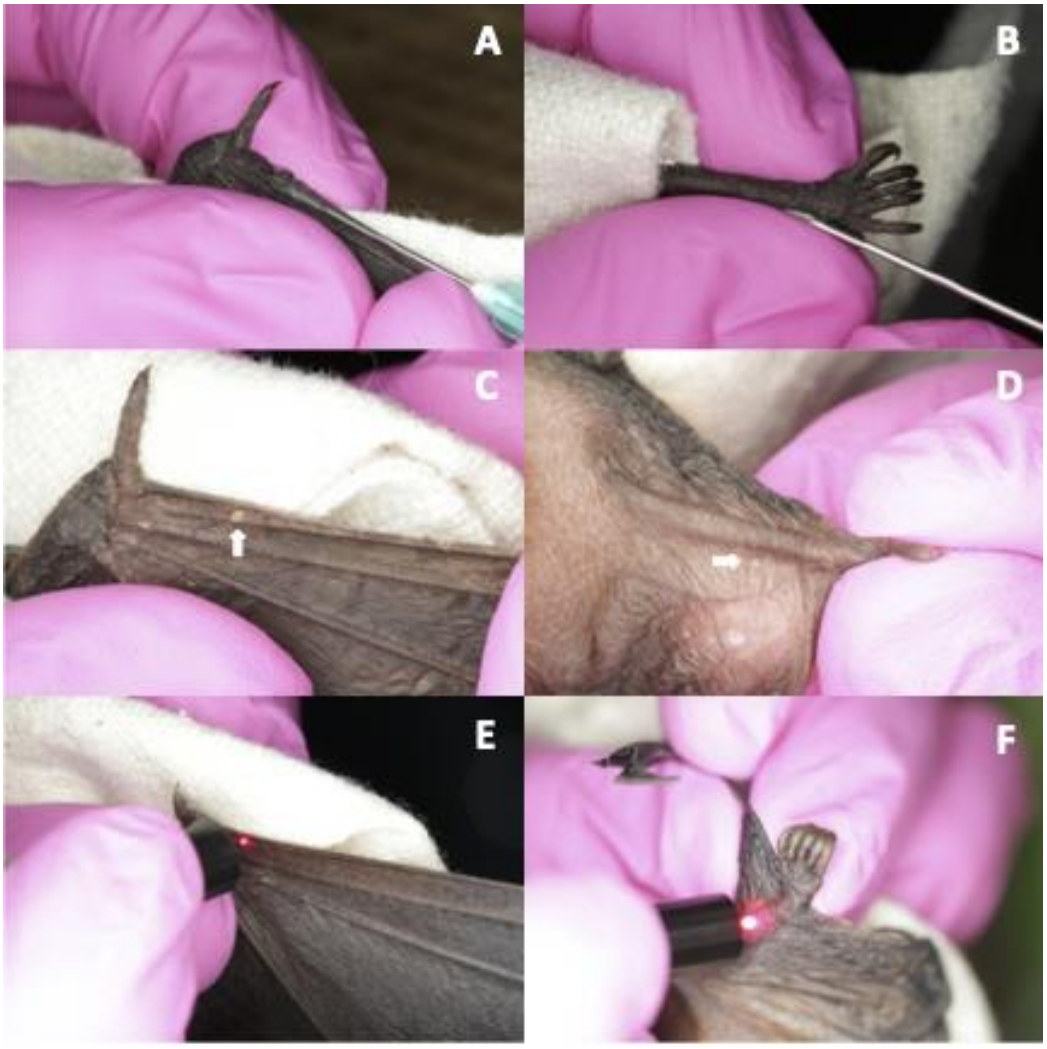

Fig. 2.1.—Subcutaneous implantation and laser scanning of P-Chips in the wing and leg of the big brown bat. (A) Injection of p-Chip parallel to the 2nd metacarpal. (B) Injection of p-Chip near the base of the foot parallel to the tibia. (C) Visibility of P-Chip against the second metacarpal and (D) in the tissue beside the tibia. The location of the P-Chip in both images is indicated by a *white arrow*. (E) Using the wand to illuminate (scan) the p-Chips implanted in the wing and (F) leg. p-Chip dimension = 500 × 500 µm.

1. wing (primary site; Fig. 2.1A, C; n = 30)—dorsally over the proximal part and parallel to the right 2nd metacarpal, approximately 1 cm from the proximal carpal joint; and
2. leg (secondary site; Fig. 2.1B, D; n= 13)—parallel to the midpoint of the right tibia along its dorsal side.

Important considerations in site selection were accessibility for implantation and later scanning with the wand, transparency of the skin for tag visibility, and minimizing risk of damaging blood vessels, nerves, or tendons during injection. Implanted p-Chips were positioned with their photocells facing outward (i.e. away from the bone and toward the exterior skin surface). Hemostatic powder and/or small ephrin balls were used to stop any bleeding observed at the injection site. Following injection, p-Chips were scanned with the laser reader wand (Model WA-4000) and the data were automatically transferred into a Microsoft Excel spreadsheet using p-Chip Reader software provided by the manufacturer (Fig. 2.1 E,F). Of 30 bats tested, 13 were tagged in both sites and the remainder were tagged in the wing only (Table 2.1).

p-Chip Scanning.—Two persons (SS, RP) conducted each scanning session. The first person, the "handler", restrained and manipulated the bat and positioned the wand to be in close proximity to the p-Chip for a successful read. The second person, the "recorder", operated the digital timer, software, and recorded data. The roles of the two individuals were randomized at the start of each session and were switched when approximately half of the bats had been recorded. After scanning, bats were returned to the husbandry facility where they

Table. 2.1.—Post-implantation day (PID) recording dates for p-Chips implanted in the wing and leg of the big brown bat, *Eptesicus fuscus*

PID #	Date (YYYY-MM-DD)	# Bats (wing only)	# Bats (wing + leg)	Total # Bats
0*	2019-11-11	17	13	30
1	2019-11-12	17	13	30
8	2019-11-19	17	13	30
15	2019-11-26	17	13	30
22	2019-12-03	16	13	29
32	2019-12-13	16	13	29
60	2020-01-10	15	13	28
74	2020-01-24	15	13	28
81	2020-01-31	15	13	28
88	2020-02-07	15	13	28
95	2020-02-14	15	13	28
464	2021-02-17	5	5	10

*PID 0 = day of p-Chip implantation

remained until the next session. A movie illustrating the procedure of p-Chip implantation and scanning in the wing of *E. fuscus* is available as Supplementary Data (see Supplementary Data SD1).

We quantified p-Chip readability separately for each implantation site by recording the time spent locating and scanning tags. After the handler removed a bat from its cage, the recorder started a digital timer to mark the start of handling time, defined as the duration (s) between the initial restraining of the bat and the end of the scanning trial. Working quickly, the handler manipulated and oriented the bat so its p-Chip implantation site in the wing or leg was accessible for scanning. At this point, the visibility of the p-Chip was assessed by the handler using a yes/no nominal scale. Once the handler picked up the wand, the recorder started a second (lap) timer to measure the p-Chip scan time for that location. The handler then directed the laser beam of the wand back and forth over the p-Chip to obtain a read.

When the laser is in close proximity to the p-Chip, the light intensity briefly increases to activate the transponder's photocells (PharmaSeq, undated white paper). In practice, these proximity "wand flashes" helped us to obtain a successful read. When the transponder's unique 9-digit ID number was detected by the p-Chip Reader software, it was automatically logged to an Excel spreadsheet and an audible tone was emitted from the computer. Following a successful read, the recorder stopped the timers. Conversely, if the read was unsuccessful, no audible tone was produced and the handler would continue scanning the implantation site. If a p-Chip was not read within 45 s of handling

time, the handler proceeded with a 2 min free scan and directed the laser beam both dorsally and ventrally, on and away from the original implantation site, as a last attempt to read a chip that may have shifted laterally (i.e., translocated) and/or reoriented and flipped *in situ* so it's photocells no longer faced outward. When a p-Chip was not read within 2 min 45 s, the tag was recorded as unreadable for that session. For bats with p-Chips in both the wing and leg, a coin flip determined which location to scan first and the bat was returned to its cage before repeating the above procedure for the other site.

We scanned bats routinely from November 2019 to February 2020, except between 13-December-2019 and 10-January-2020 (Table 2.1). Owing to the COVID-19 pandemic, no data were collected from February 2020 until February 2021 when a subsequent recording session was conducted on PID 464, approximately 1 year later. For each trial, we recorded: (1) handling time (s), (2) scan time (s), (3) number of wand flashes (a proxy for scan attempts), (4) p-Chip visibility (yes/no), and (5) comments on the bat's overall condition. Note: we did not record handling time for the tibia on PID 0 and p-Chip visibility was recorded starting on PID 22.

Data Analyses.—Data analysis was conducted in R (R Core Team, 2021) and visualized with the *ggplot2* (Wickham, 2016), *plotrix* (Lemon, 2006), and *ggbreak* (Xu et al. 2021) packages. Unless stated otherwise, summary data are displayed as the mean ± standard error (*SE*), with applicable measures reported with 95% confidence intervals (CI). Pearson's product-moment correlation (*r*) evaluated the relationship between handling time and scan time. Two-sample *t*-

tests were used to compare handling and scan times between handlers. Dependent variables were evaluated quantitatively with generalized linear mixed-effects models (GLMMs) that included tag Location (leg vs. wing) and Day as fixed effects and an intercept for each bat as a random effect. Specifically, the models for handling time and scan time were fit to the data using the *lmer* function, whereas p-Chip visibility, number of wand flashes, and the proportion of unreadable p-Chips were modeled using the *glmer* function in the *lme4* and *lmerTest* packages (Bates et al. 2015; Kunznestova et al. 2017). We excluded the PID 464 data to ensure the GLMM analyses were not skewed by an extreme value. The main effects of Day and Location, and the Day x Location interactions for handling time and scan time were evaluated with *F* tests using degrees of freedom calculated with Satterthwaite's method (Satterthwaite, 1946). By contrast, the fixed effects for p-Chip visibility, wand flashes, and unreadable p-Chips were evaluated with Chi-square (χ^2) tests computed by the *Anova* function in the *car* package (Fox and Weisberg, 2019). The GLMMs for the binomial variables p-Chip visibility and unreadable p-Chips were fit using the *logit* link-function, whereas the model for the continuous variable number of wand flashes was fit using a Poisson regression with a *log* link-function. The models for every variable fit the data reasonably well and we show best-fitting curves for each Location and variable (Fig. 2.2–2.6).

Results

To evaluate scanning efficacy, we compared bat handling times (Fig. 2.2) and p-Chip scanning times (Fig. 2.3) for the wing and leg implantation sites. By

definition, handling time was always larger than the respective scan time, and the two paired measures were strongly positively correlated (r = 0.916, t_{388} = 44.85, P < 0.001, 95% CI [0.90, 0.93]).

Handling Time.—Handling times were, on average, longer and more variable when recording p-Chips in the leg versus the wing (Fig. 2.2). The distribution of handling times contained outliers and was positively skewed (range = [3, 255], median = 22, mean = 47.1), hence we analyzed log-transformed data. The main effect of Location was significant ($F_{1,369}$ = 19.1, P < 0.001), but the main effect of Day ($F_{1,346}$ = 0.26, P = 0.61) and the Location x Day interaction ($F_{1,346}$ = 0.38, P = 0.54) were not. Similar results were obtained when we analyzed non-transformed handling time. In summary, handling time was significantly longer when recording p-Chips in the leg versus the wing, and this finding did not vary over the course of the study.

We also compared handling times between the two bat handlers. The average handling time to record p-Chips implanted in the wing was 39 and 26 s for the two handlers, and this difference was significant ($t_{244.36}$ = 4.36, P < 0.001, 95% CI [8, 20]]). The mean handling time to record p-Chips implanted in the leg was 83 and 75 s for each handler, but this difference was not significant ($t_{106.63}$ = 0.57, P = 0.573, 95% CI [-20, 37]).

Scan Time.—Scan times were less variable for p-Chips implanted in the wing versus the leg (Fig. 2.3). Similar to handling time, the distribution of data for scan time contained outliers and was positively skewed (range = [1, 157], median = 5, mean = 16.3), thus we analyzed log-transformed data. There was no main

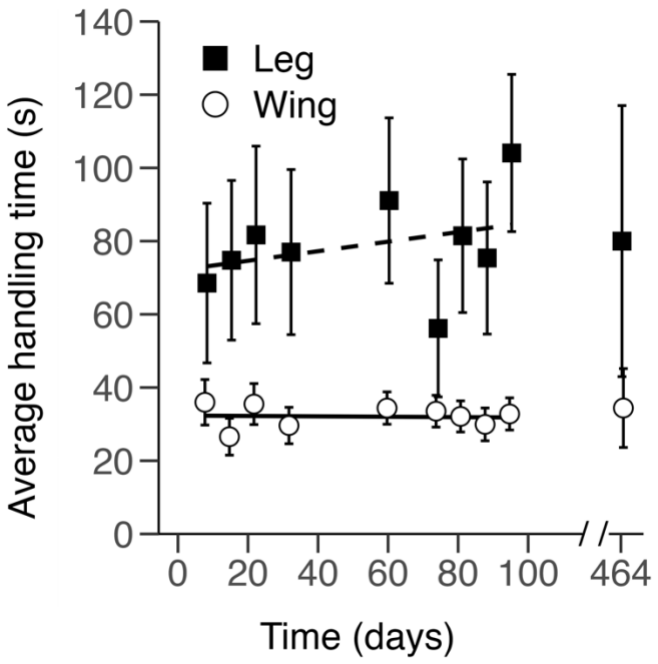

Fig. 2.2.—Bat handling times per recording day for p-Chips implanted in the wing and leg. Mean ± *SE* handling times were measured separately for p-Chips implanted in the second metacarpal (wing, n = 30) and tibia (leg, n =13) from PID 8 to PID 95, with a subsequent recording session ~1 year later on PID 464. *Dotted* and *dashed lines* represent the best-fitting, mixed-model regression lines for p-Chips implanted in the wing (*open circles*) and leg (*closed squares*). For data points collected on the same day, the markers have been displaced ±0.3 along the *x-axis* for clarity.

effect of Location ($F_{1,367}$ = 0.86, P = 0.35), hence scan times for p-Chips implanted in the wing and leg were similar (Fig. 2.3). However, the main effect of Day ($F_{1,342}$ = 15.1, P < 0.001) was significant; average scan times increased between PID 1 and PID 95 for p-Chips implanted in both the wing and leg. The increase in scan time across days was slightly greater for p-Chips located in the leg (0.8% per day) compared to the wing (0.5% per day), but the Location x Day interaction was not significant ($F_{1,342}$ = 0.76, P = 0.38). An analysis of non-transformed scan time data yielded similar results, except that analysis also found a significant Location x Day interaction ($F_{1,343}$ = 6.27, P < 0.013). Unlike the result for handling time, our analysis failed to find a difference in scan time for p-Chips implanted in the wing and leg. Instead, we found evidence for a small but significant increase in scan time from PID 1 to PID 95 that may be slightly greater for p-Chips implanted in the leg. There was no difference in scan times between the two bat handlers for p-Chips located in the wing ($t_{240.67}$ = 0.71, P = 0.479, 95% CI [-3, 7]) and leg ($t_{65.55}$ = -0.66, P = 0.512, 95% CI [-23, 12]).

p-Chip Visibility.—Compared to the skin of the leg, the bat wing membrane is thinner, less opaque, and sits tightly on the digits, hence there is less room for p-Chips to become displaced or flip at the implantation site. For these reasons, we expected p-Chips to remain more visible in the wing than in the leg. The visibility of p-Chips in the wing was initially close to 100% and only decreased to ~70% between PID 22 and PID 95 (Fig. 2.4). In contrast, less than half of the p-Chips implanted in the leg were visible on PID 22, a percentage that remained relatively constant over time (Fig. 2.4). The main effect of tag Location

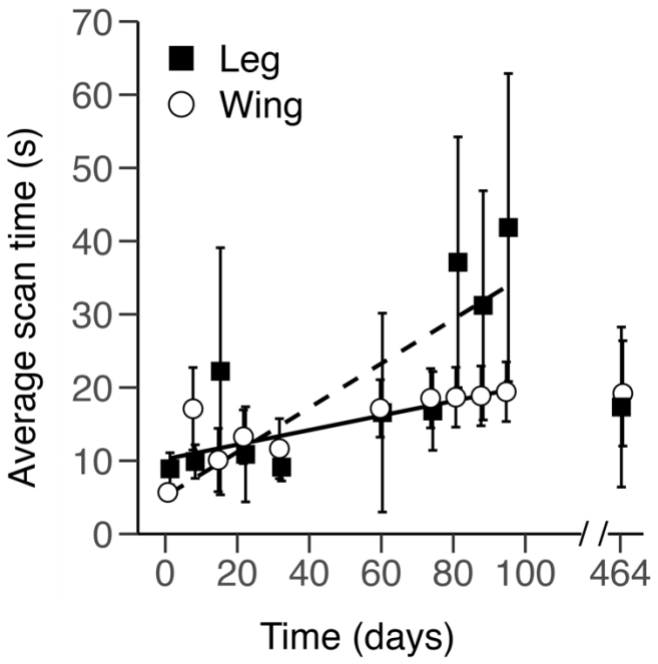

Fig. 2.3.—Scan times per recording day for p-Chips implanted in the wing and leg. Mean ± *SE* scan times were recorded separately for p-Chips implanted in the second metacarpal (wing, n = 30) and tibia (leg, n =13) from PID 1 to PID 95, with a subsequent recording session ~1 year later on PID 464. Data do not include occurrences of unsuccessful p-Chip reads when the maximum scan time was reached (165 s). *Dotted* and *dashed lines* represent the best-fitting, mixed-model regression lines for p-Chips implanted in the wing (*open circles*) and leg (*closed squares*). For data points collected on the same day, the markers have been displaced ±0.3 along the *x-axis* for clarity.

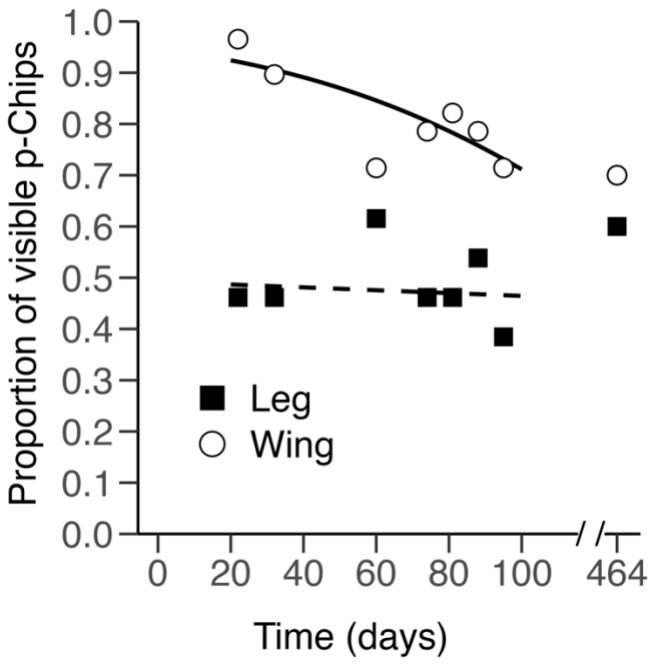

Fig. 2.4.—Tag visibility per recording day for p-Chips implanted in the wing and leg. Data illustrate the proportion of p-Chips implanted in the second metacarpal (wing, n = 30) and tibia (leg, n = 13) that were visible to the naked eye from PID 22 to PID 95, with a subsequent recording session ~1 year later on PID 464. Visibility measured according to the hander's subjective judgement using a nominal Yes/No scale. *Dotted* and *dashed lines* represent the best-fitting, mixed-model regression lines for p-Chips implanted in the wing (*open circles*) and leg (*closed squares*).

was significant ($\chi^2 = 26.78$, *d.f.* = 1, $P < 0.001$); visibility was greater for p-Chips implanted in the wing compared to in the leg (Fig. 2.4). There was no main effect of Day ($\chi^2 = 3.44$, *d.f.* = 1, $P = 0.064$) and the Location x Day interaction ($\chi^2 = 2.75$, *d.f.* = 1, $P = 0.097$) was also nonsignificant. Given the trends in our data (Fig. 2.4), the failure to find a Location x Day interaction was surprising. We therefore decided to examine the effect of Day separately for each Location and found a significant effect for p-Chips implanted in the wing ($\chi^2 = 6.09$, *d.f.* = 1, $P = 0.014$) but not in the leg ($\chi^2 = 0.02$, *d.f.* = 1, $P = 0.88$).

Wand Flashes.—The average number of wand flashes decreased by ~47% in the wing and ~82% in the leg between PID 1 and PID 95 (Fig. 2.5). The main effects of Location ($\chi^2 = 6.02$, *d.f.* = 1, $P = 0.014$) and Day ($\chi^2 = 99.32$, *d.f.* = 1, $P < 0.001$) were significant. The Location x Day interaction ($\chi^2 = 4.83$ *d.f.* = 1, $P = 0.023$) was also significant, with the effect of day being smaller for p-Chips implanted in the leg. A follow-up analyses examining the effect of Day separately for each Location found a significant effect of Day for p-Chips implanted in both the wing ($\chi^2 = 55.65$, $P < 0.001$) and in the leg ($\chi^2 = 49.35$, $P < 0.001$).

p-Chip Readability.—Over the course of our experiment, there were zero instances of unreadable p-Chips in the wing (Fig. 2.6). In contrast, ~23% of p-Chips implanted in the leg were unreadable on PID 1—one day after implantation—and this doubled to 46% by PID 95 (Fig. 2.6); however, the effect of Day was not significant ($\chi^2 = 0.56$, *d.f.* = 1, $P = 0.45$).

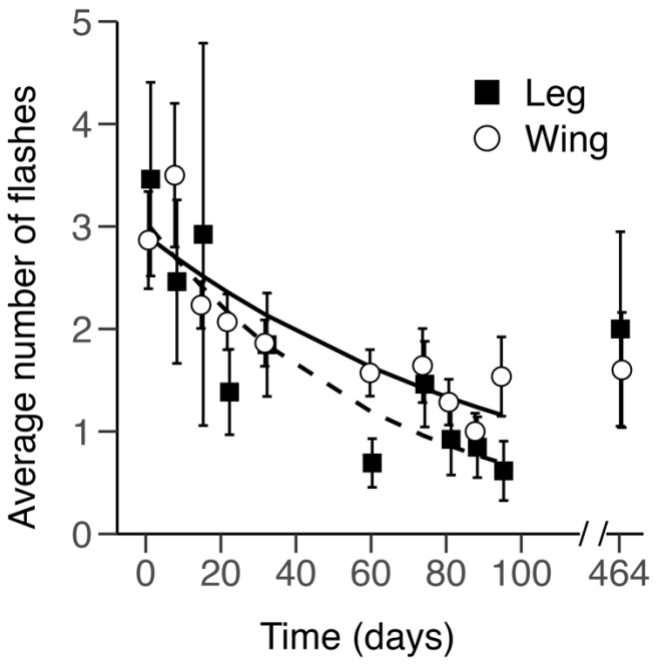

Fig. 2.5.—Wand flashes per recording day for p-Chips implanted in the wing and leg. Shown are the mean ± *SE* number of wand flashes recorded in p-Chips implanted in the second metacarpal (wing, n = 30) and tibia (leg, n = 13), prior to a successful p-Chip read from PID 1 to PID 95, with a subsequent recording session ~1 year later on PID 464. *Dotted* and *dashed lines* represent the best-fitting, mixed-model regression lines for p-Chips implanted in the wing (*open circles*) and leg (*closed squares*). For data points collected on the same day, the markers have been displaced ±0.3 along the *x-axis* for clarity.

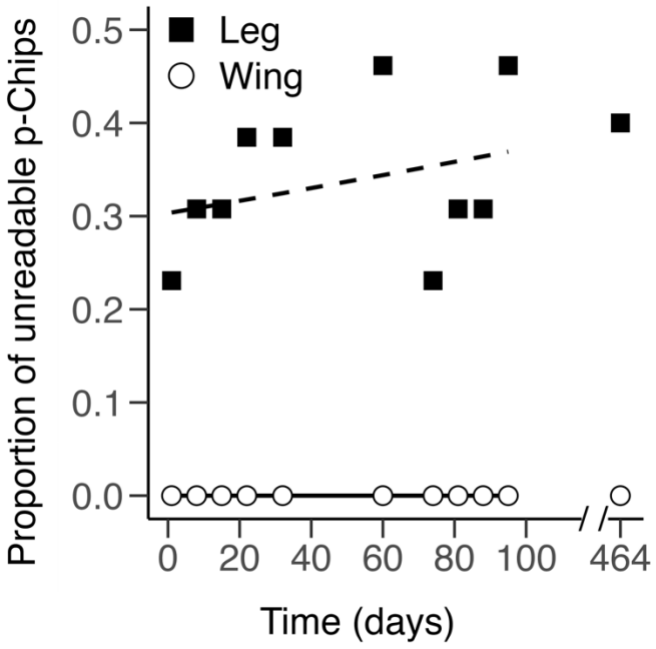

Fig. 2.6.—Unreadable tags per recording day for p-Chips implanted in the wing and leg. Shown are the proportion of unreadable p-Chips in the second metacarpal (wing, n = 30) and tibia (leg, n = 13) over the duration of the study. *Dotted* and *dashed lines* represent the best-fitting, mixed-model regression lines for p-Chips implanted in the wing (*open circles*) and leg (*closed squares*).

All p-Chips were injected with their photocells facing outward yet we recorded 67 instances where the orientation of the tag had flipped, as confirmed by obtaining a successful read by scanning the ventral surface of the wing (n = 54) or the opposite side of the leg (n = 13). In the subset of 13 bats with tags in both the wing and leg, for each animal we counted the number of days, between PID 1 and PID 95 (n = 10 days total), with a successful ventral scan for each location. The mean ± *SD* proportion of days with a successful ventral scan in the wing (0.16 ± 0.28, n = 21 flips) and leg (0.10 ± 0.16, n = 13 flips) did not differ (t_{12} = 0.63, *P* = 0.544, 95% CI [-0.15, 0.28]). In one bat that died after our study concluded, we could not read its p-Chip in the leg using any wand orientation so we dissected the patagium around the tibia and visually confirmed that a "chip flip" had occurred *in situ* and that the tag was still readable.

Animal Health.—During implantation, we observed instances of bleeding that were promptly stopped with hemostatic powder and/or small ephrin balls. Routine health checks throughout our study found instances of scar tissue buildup around injection sites, but we saw no obvious effects of p-Chip implantation on bat behaviour or health. Some bats developed dry skin and/or hair loss, but these changes occur seasonally among bats in the captive colony and thus were not directly associated with tag implantation or animal handling. Our sample size decreased over time because 20 bats died from an unknown cause, mainly from November 2020 to February 2021. To our knowledge, these deaths were not associated with tag implantation or handling because no data were collected

during this time, no inflammation was observed at the implantation sites, and bats without p-Chips also succumbed to illness.

Discussion

Overall, the results of our study suggest that p-Chips are a feasible bat marking technique and that, of the two implantation sites we tested, the second metacarpal is preferred due to the relative ease and efficiency of locating and scanning the microtransponder. Below we discuss the rationale for this conclusion in more detail.

Handling Time.—The two persons collecting data were experienced bat handlers, with one (RP) having shorter handling times for scanning tags in the wing but not the leg. Handling times remained fairly consistent throughout the study (Fig. 2.2) but were shorter when scanning p-Chips embedded in the wing versus the leg, likely because it was easier for handlers to open the restrained bat's wing and expose its metacarpal compared to manipulating and holding its tibia.

Scan Time.—Average scan times increased from PID 1 to PID 95 for p-Chips in both the wing and leg but did not differ between the two implantation sites (Fig. 2.3). Scanning may be hampered by a variety of factors, such as transponder translocation away from the original implantation site and/or the p-Chip's photocells becoming obscured from the wand, for example, by flipping *in situ* so they no longer face outward or as a result of connective tissue buildup around the implant as a foreign body.

p-Chip Visibility.—Tags implanted in the leg were less visible compared to those implanted in the wing (Fig. 2.4), likely because the skin of the uropatagium in *E. fuscus* is darker, thicker, and looser around the tibia. Tag visibility is important; it increases the accuracy of wand positioning and in turn contributes to scanning efficiency. The visibility of subcutaneous tags may be impacted by the deposition of scar tissue at the injection site. Together, these factors may have interfered with the ability of the laser to activate the tag's photocells, resulting in a higher proportion of unreadable p-Chips implanted in the leg compared to the wing (Fig. 2.6). This may have further contributed to longer handling times for bats with p-Chips in the leg (Fig. 2.2).

Wand Flashes.—The number of wand flashes can be used as a proxy measure of unsuccessful reading attempts. The number of wand flashes decreased over the study for the wing and leg implantation sites (Fig. 2.5). There was also a small difference in the number of wand flashes for a successful p-Chip read between these sites. This latter result was unsurprising given the large differences in the proportions of visible tags (Fig. 2.4) and successful reads (Fig. 2.6) between the wing and leg. The decrease in number of wand flashes over time likely resulted from increased user experience (i.e. practice positioning the wand and scanning chips).

p-Chip Readability.—The readability of p-Chips differed markedly between the wing and the leg (Fig. 2.6). All transponders implanted in the wing remained readable, whereas the proportion of readable p-Chips in the leg was lower and more variable over time. This finding is consistent with the lower

visibility of p-Chips in the leg (Fig. 2.4). Re-orientation of p-Chips at the implantation site is known to influence reading success. For example, in laboratory mice post-mortem histology found that p-Chip reorientation renders tags unreadable when the photocells face the tail vertebrae (Gruda et al. 2010). This is in contrast to subcutaneous PIT tags which can change orientation in the animal after implantation but without loss of function; however, readability can still be impacted when PIT tags translocate to an unexpected location and users determine the tag is lost (Prentice and Park, 1983, Gibbons and Andrews, 2004). In some bats we attempted to manually flip the orientation of the p-Chip *in situ* but were unsuccessful. There were other instances when p-Chips appeared to reorient several times within the skin so that the transponder was successfully scanned dorsally, then ventrally, and then again dorsally across sessions. We speculate that tag translocation and/or chip flipping is more frequent in thick, loose skin that allows more room for p-Chip movement (e.g., the uropatagium). To alleviate this, we encourage manufacturers to design microtransponders with omnidirectional reading capabilities (e.g. Mikhailovskaya et al. 2021).

Animal Health.—Handling by humans can stress bats, particularly during trapping or when they are torpid, and adverse effects of handling are associated with the method of tagging (Barclay and Bell, 1988; Kunz and Weise, 2009). Our bats were from a captive colony, used to regular handling, and typically remained calm during p-Chip implantation and subsequent scanning trials, suggesting that our protocol did not adversely affect them. Some bats bled at the injection site immediately following implantation but this was easily and quickly treated. In a

field study of the world's smallest bat, p-Chips were implanted in 277 Kitti's hog-hosed bat (*Craseonycteris thonglongyai*) with no signs of damage or inflammation in 70 recaptured individuals (Ngamprasertwong et al. 2022). In mice, marking with p-Chips is thought to minimize implantation stress owing to the tag's small size (Gruda et al. 2010).

Comparison Between Marking Techniques.—Table 2.2 summarizes and compares the characteristics of split-ring bands, PIT tags, and p-Chips used to mark bats. Relative to conventional forearm bands and PIT tags, p-Chips are much smaller. They also require a smaller diameter injection needle than PIT tags (PIT tag: 12-gauge, outer diameter = 2.769 mm; p-Chip: 21-guage, outer diameter = 0.819 mm, Biomark, Boise, ID, USA; https://www.biomark.com), which in turn can be expected to pose less risk to animal health. Because PIT tags require a large injection needle they are more susceptible to expulsion from the body via the puncture site. By contrast, we noticed only one instance where a p-Chip was expelled during implantation. Bats can damage (i.e., make illegible) and/or remove plastic split-ring bands by chewing on them.

Scanners used to read p-Chips and PIT tags differ in notable ways. Critically, PIT tag readers have less stringent proximity and orientation requirements. The p-Chip laser wand we used (model WA-4000) must be within <8 mm of the implant whereas PIT tag readers can work at distances of 45-500 mm, depending on the model. The hand-held readers for PIT tags and p-Chips also differ in usability. Many different PIT tag scanner models exist, with some portable (e.g. pocket scanners), some stationary (e.g. circular antenna installed at

Table. 2.2.—Features of split-ring bands, PIT tags, and p-Chips for marking bats. Information on bands / PIT tags comes from many studies whereas for p-Chips it is based mainly on this report.

Tag Characteristic	Split-Ring Bands	PIT tags	p-Chips
Composition	plastic, metal	glass capsule	semi-conductor
Invasive Application?	no (external)	yes (subcutaneous)	yes (subcutaneous)
USDA/CCAC Rating	Category B	Category C	Category C
Pain/Duration	little-to-none/short	minor/short	minor/short
Application Tool?	banding tool/pliers; by hand	sterile needle (12-16 G)	sterile needle (21 G)
Application Injury?	no (unlikely)	yes (bleeding); internal organ damage, death (rare)	yes (bleeding); possible limb or tendon damage, infection
Post-Application Morbidity/Mortality	short- and long-term skin irritation (inflammation or infection); restricted circulation/death (rare)	inflammation, infection / death (rare)	possible inflammation, infection/not reported
Affects Behavior?	yes (bats may scratch or chew band)	not reported	not reported
Location	forearm (typical) thumb or leg (atypical)	nape/back (between shoulder blades)	no standard location*
Code	analog (engraved on band)	digital RFID (alphanumeric code)	digital RFID 9-digit (alphanumeric code)
Size	2 to >6 mm diameter	1 to 4 mm diameter; 8 to 32 mm length	500 × 500 × 100 µm (l × w × h)
Bat Size Restriction?	none	none	not tested (likely none)
Removable?	yes (also by the bats)	no (requires surgery)	no (requires surgery)
Reusable?	yes	yes (uncommon; requires sterilization)	not tested; (requires sterilization)
Reader	visual inspection	built-in display or wireless connection	laser wand USB connected to computer)
Reader Range	~0.5 m (by eye)	≤500[§] mm	≤10 mm
Reader Orientation	band surface	N/A	chip surface with photocell
Visible?	yes (bat must be in hand to read unique number)	no (under skin/fur)	yes (varies with skin pigmentation)
Persistence	lifetime (bats can damage by chewing)	lifetime	lifetime (but tag can flip and be obscured *in situ*)
Tag Cost	<$1.00 USD	≤$10.00 USD	$2.00 USD
Reader Cost	N/A	$300-$2000 USD	$2000 USD
Availability/ Compatibility	multiple suppliers/ cross compatible	multiple suppliers/ not all cross compatible	p-Chip Corp./ internally compatible
Field Tested?	yes	yes no	

*results of present study suggest 2nd metacarpal as a prospective location for small-to-medium-sized bats

[§]varies with tag and reader model; automated readers can be mounted at roost entrances or on a pole to scan clusters of bats

animal entrance/exit points), and others designed to work as arrays to increase the effective reading range. Similar scanner designs may be challenging to incorporate for p-Chips because the photocells are located on one surface of the tag and require precise alignment with the reading wand. Furthermore, not every PIT tag can be scanned by every PIT reader because both must function on the same radio frequency to communicate with one another (Gibbons and Andrews, 2004). In contrast, the p-Chip technology is proprietary and users rely on a sole source supplier. Use of the p-Chip wand obligates connecting to a computer to record transponder ID numbers whereas PIT tag readers typically have a built-in display. Lastly, there are significant cost differences between p-Chip and PIT tag technologies (Jolley-Rogers et al. 2012). Although individual p-Chips are less expensive to deploy than PIT tags (Smyth and Nebel, 2013), the cost of a p-Chip laser reader wand is higher than most PIT tag readers (Table 2.2).

The use of any marking method comes with risks. Despite miniaturization leading to low invasiveness, and potentially minimal impact on animal health and wellbeing, using p-Chips to mark bats poses a set of operational challenges, mostly related to locating and reading the implanted transponder. For example, we know p-Chips remain visible in the bat wing for at least~1.3 years, but their permanence beyond this is unknown. Our work in captive bats did not record instances of unreadable p-Chips in the wing (Fig. 2.6) and ca. 70% of these tags remained visible over time (Fig. 2.4). The reduced visibility of p-Chips implanted in the leg increased the time to find and scan them (Fig. 2.3). We noticed instances where a p-Chip in the leg was deemed unreadable one day but gave a

viable read on a subsequent day (n = 9). While it is possible for p-Chips to be expelled from the body, which would affect estimates of marked versus unmarked individuals, we recorded only one instance of tag loss. Retention of p-Chips and PIT tags has been examined and compared in different fish species (Chen et al. 2013; Faggion et al. 2020, Moore and Brewer, 2021).

Other Considerations.—Researchers working with tagged insects have obviated the need for handling by placing p-Chips in highly visible and standardized locations (Jolley-Rogers et al. 2012), or by designing housing to guide insects through narrow spaces for efficient wand reading (Robinson et al. 2009; Robinson and Mandecki 2011). Several studies have developed similar approaches for automated PIT tag reading in bats crawling through entrances to roosts or hibernacula (e.g., Silvy et al. 2012; Britzke et al. 2014; Norquay and Willis 2014). For now, using p-Chips for marking bats may be restricted to situations when animals are directly handled.

The ability to distinguish marked and unmarked animals is vital in recapture studies of free-ranging populations. Mark-recapture work requires tags that persist and remain visible/detectable, ideally over the animal's lifespan. Compared to external tags for marking bats (see Kunz and Weise, 2009), p-Chips are highly inconspicuous. This reinforces the importance of standardizing the implantation site when considering the wider adoption of p-Chips to mark bats, as in laboratory mice (Gruda et al. 2010) and fish (Moore and Brewer 2021).

Our results support the conclusion that the relatively translucent, thin, and tighter skin surrounding the second metacarpal of *E fuscus* is a better p-Chip implantation site compared to the darker (opaque), thicker, and looser skin of the uropatagium around the tibia. But these characteristics will vary in other bat species, depending on their size and morphology. For example, the second metacarpal may be an unfeasible implantation site in bats smaller than *E. fuscus* because the gauge of the needle may exceed the width of the bone and this could tear the chiropatagium. In smaller-bodied bats, like *Craseonycteris,* implanting p-Chips in the forearm may be feasible. On the other hand, in larger bats with robust skin, like *Artibeus, Phyllostomus,* or *Cynopterus*, locating and scanning forearm p-Chips may be problematic. Because tail anatomy differs markedly among bat families—in many species the tail moves freely within the uropatagium while in others it is completely lacking, plus some bats have a densely haired uropatagium—this renders the tail as an impractical site for implantation. Ultimately, researchers may have to designate taxon-specific standard sites for implanting p-Chips in Chiroptera.

Despite the above caveats, the feasibility of p-Chips must be field-tested in different species of free-ranging bats, preferably in settings where there is high likelihood of recapturing individuals. For now, we recommend pairing p-Chips with another marking method—such as bands or PIT tags—or marking animals with two p-Chip transponders (e.g., one in each wing) to aid in the assessment of tag visibility, readability, retention, and localization over time.

While the results of our pilot study are encouraging and warrant further field testing, *we caution researchers against using p-Chips as the sole method for marking bats at this time*, because the consistency of applying this proprietary technology across bat taxa and in different settings remains unknown, which could pose risks to long-term data integrity. Since revising this manuscript our original laser wand (model WA-4000) was recalled by the p-Chip Corp and replaced with a newer model (WA-6000) to comply with regulations for Class 3R laser products from the Center for Devices and Radiological Health. The new model has reduced laser pulse power, emits fewer pulses during tag reading, and has a smaller spot size, but is reported to activate p-Chips at a longer distance (up to 15 mm). We conducted a preliminary test with the upgraded wand on six thawed *E. fuscus* cadavers from our original study and two recently tagged live individuals, and observed variation in scanning performance between two operators. The decrease in laser spot size and pulse emissions may reduce the efficiency of scanning subcutaneous p-Chips, especially when the tags are not visible. We suggest that researchers experimentally evaluate the scanning efficiency of the new WA-6000 wand in bats, using an approach similar to ours, before deploying p-Chips in the field.

Acknowledgements

Research supported by Discovery Grant RGPIN-2020-06906 to P.A.F. from the Natural Sciences and Engineering Research Council of Canada. We thank Lucas Greville, Doreen Möckel, Renata Soljmosi, Tom Groulx, Taylor Byron, and Emily Wuerch for assistance with p-Chip recording, Dr. Kathleen Delaney, Dawn

Graham, and the staff of the Psychology Animal Facility for veterinary and animal care support, and the p-Chip Corporation for advice and resources.

Supplementary Data

Supplementary Data SD1.—Movie illustrating subcutaneous implantation and laser wand reading of a p-Chip injected along the dorsal surface of the 2nd metacarpal in the right wing of a yearling big brown bat (*Eptesicus fuscus*). Also shown are instances of successful laser wand reads accompanied by an audible beep and data output to the computer, and unsuccessful tag reads with no beep or data output.

Literature Cited – Chapter 2: Scanning efficacy of p-Chips implanted in the wing and leg of the big brown bat (*Eptesicus fuscus*)

Barker G. B., Lumsden L. F., Dettmann E. B., Schedvin N. K., Schulz M., Watkins D., Jansen L. 2001. The effect of forearm bands on insectivorous bats (Microchiroptera) in Australia. Wildlife Research 28:229–237.

Barnard S. M. 1989. The use of microchip implants for identifying big brown bats (*Eptesicus fuscus*). Animal Keepers Forum 16:50–52.

Barclay R. M. R., Bell G. P. 1988. Marking and observational techniques. In: Kunz T.H., editor. Ecological and behavioral methods for the study of bats. Smithsonian Institution Press; p. 59–76.

Bates D., Mächler M., Bolker B., Walker S. 2015. Fitting linear mixed-effects models using lme4. Journal of Statistical Software 67:1–48.

Bonaccorso F. J., Smythe N., Humphrey S. R. 1976. Improved techniques for marking bats. Journal of Mammalogy 57:181–182.

Bradbury, J. W. (1977). Lek mating behaviour in the hammer-headed bat. Zeitschrift für Tierpsychologie, 45(3), 225-255.

Britzke E. R. Gumbert M. W. Hohmann M. G. 2014. Behavioural response of bats to passive integrated transponder tag reader arrays placed at cave entrances. Journal of Fish and Wildlife Management 5:146–150.

Buchler E. R. 1976. A chemiluminescent tag for tracking bats and other small nocturnal animals. Journal of Mammalogy 57:173–176.

Campbell P., Reid N. M., Zubaid A., Adnan A. M., Kunz T. H. 2006. Comparative roosting ecology of *Cynopterus* (Chiroptera: Pteropodidae) fruit bats in peninsular Malaysia. Biotropica 38:725–734.

Chaverri G., Quirós O. E., Kunz T. H. 2007. Ecological correlates of range size in the tent-making bat *Artibeus watsoni.* Journal of Mammalogy 88:477–486.

Chen C. H., Durand E., Wang J., Zon L. I., Poss K. D. 2013. Zebrafish transgenic lines for in vivo bioluminescence imaging of stem cells and regeneration in adult zebrafish. Development 140:4988–4997.

Cockrum E. L. 1956. Homing, movements, and longevity of bats. Journal of Mammalogy 37:48–57.

Delcourt J., Ovidio M., Denoël M., Muller M., Pendeville H., Deneubourg J-L., Poncin, P. 2018. Individual identification and marking techniques for zebrafish. Reviews in Fish Biology and Fisheries 28:839–864.

Dietz, C., Dietz, I., Ivanova, T., and Siemers, B. M. 2006. Effects of forearm bands on horseshoe bats (Chiroptera: Rhinolophidae). Acta Chiropterologica, 8(2), 523-535.

Dwyer P. D. 1966. Observations of *Chalinolobus dwyeri* (Chiroptera: Vespertilionidae) in Australia. Journal of Mammalogy 47:716–718.

Dwyer P. D. 1969. Population ranges of *Miniopterus schreibersii* (Chiroptera) in southern Australia. Australian Journal of Zoology 17:675–686.

Dwyer P. D. 1970. Social organization in the bat *Myotis adversus.* Science 168:1006–1008.

Faggion S., Sanchez P., Vandeputte M., Clota F., Vergnet A., Blanc M. O., Allal F. 2020. Evaluation of a European sea bass (*Dicentrarchus labrax L.*) post-larval tagging method with ultra-small RFID tags. Aquaculture 520:734945.

Flemming T. H., Eby P. 2003. Ecology of bat migration. In: Kunz T.H., Fenton M.B., editors. Bat ecology. University of Chicago Press; p. 156–208.

Fox J., Weisberg S. 2019. An R companion to applied regression, third edition. Sage, Thousand Oaks CA.

Gibbons J. W., Andrews K. M. 2004. PIT tagging: simple technology at its best. BioScience 54:447–454.

Goldshtein A., Harten L., Yovel Y. 2021. Mother bats facilitate pup navigation learning. Current Biology 32, 350–360.

Greenhall, A. M., and Paradiso, J. L. 1968. Bats and bat banding. US Department of the Interior, Fish and Wildlife Service, Bureau of Sport Fisheries and Wildlife, Resource Publication 72.

Gruda M. C., Pinto A., Craelius A., Davidowitz H., Kopacka W., Li J., Qian J., Rodriguez E., Mandecki W. 2010. A system for implanting laboratory mice with light-activated microtransponders. Journal of the American Association for Laboratory Animal Science 49:826–831.

Hamilton A. R., Traniello I. M., Ray A. M., Caldwell A. S., Wickline S. A., Robinson G. E. 2019. Division of labor in honey bees is associated with transcriptional regulatory plasticity in the brain. Journal of Experimental Biology 222: jeb200196.

Herried C. F., Davis R. B., Short H. L. 1960. Injuries due to bat banding. Journal of Mammalogy41:398–400.

Hitchcock H. B. 1965. Twenty-three years of bat banding in Ontario and Quebec. Canadian Field-Naturalist 79:4–14.

Hoyle S. D., Pople A. R. Toop G. J. 2001. Mark-recapture may reveal more about ecology than about population trends: demography of a threatened ghost bat (*Macroderma gigas*) population. Austral Ecology 26:80–92.

Humphrey S. R. 1971. Population ecology of the little brown bat, *Myotis lucifugus*, in Indiana and north-central Kentucky. Doctoral Dissertation, Oklahoma State University, Stillwater, OK, USA.

Jolley-Rogers G., Yeates D. K., Croft J., Cawsey E. M., Suter P., Webb J., Morris R. G., Qian Z., Rodriguez E., Mandecki W. 2012. Ultra-small RFID p-Chips on the heads of entomological pins provide an automatic and durable means to track and label insect specimens. Zootaxa 3359:31–42.

Kunz T. H., Hood W. H. 2000. Parental care and postnatal growth in the Chiroptera. In: Crichton E.G., Krutzsch P.H., editors. Reproductive biology of bats. Academic Press; p. 415–468.

Kunz T. H., Stern A. A. 1995. Maternal investment and post-natal growth in bats. Symposia of the Zoological Society of London 67:123–138.

Kunz T. H., Weise C. D. 2009. Methods and devices for marking bats. In: Kunz T.H., Parsons S., editors. Ecological and behavioural methods for the study of bats. 2nd Edition. The John Hopkins University Press; p. 36–56.

Kuznetsova A., Brockhoff P. B., Christensen R. H. B. 2017. lmerTest package: Tests in linear mixed effects models. Journal of Statistical Software 82:1–26.

Leigh E. G., Handley C. O. Jr. 1991. Population estimates. In: Handley C.O. Jr., Wilson D.E., Gardner A.L., editors. Demography and natural history of the common fruit bat, *Artibeus jamaicensis,* on Barro Colorado Island, Panamá. Smithsonian Contributions to Zoology No. 511; p. 77–87.

Lemon J. 2006. Plotrix: a package in the red-light district of R. R-News 6:8–12.

Mandecki W., Rodriguez E., Drawbridge J. 2016. Tagging of individual embryos with electronic p-Chips. Biomedical Microdevices 18:1-6.

Mandecki W., Kopacka W. M., Qian Z., Ertwine V., Gedzberg K., Gruda M., Reinhardt D., Rodriguez E. 2017. Tagging of test tubes with electronic p-Chips for use in biorepositories. Biopreservation and Biobanking 15:293–304.

McCracken G. F. Wilkinson G. S. 2000. Bat mating systems. In: Crichton E.G., Krutzsch P.H., editors. Reproductive biology of bats. Academic Press; p. 321–362.

Mikhailovskaya A., Yusupov I., Dobrykh D., Krasikov S., Shakirova D., Bogdanov A., Filonov D., Ginzburg P. 2021. Omnidirectional miniature RFID tag. Applied Physics Letters 119:033503.

Mohr C. E. 1934. Marking bats for later recognition. Proceedings of the Pennsylvania Academy of Science 8:26–30.

Moore D. M., Brewer S. K. 2021. Evaluation of visual implant elastomer, PIT, and p-Chip tagging methods in small-bodied minnow species. North American Journal of Fisheries Management 41:1066–1078.

Murray D. L., Fuller M. R. 2000. A critical review of the effects of marking on the biology of vertebrates. Research Techniques in Animal Ecology: Controversies and Consequences 1:15–64.

Neubaum D. J., Neubaum M. A., Ellison L. E., O'Shea T. J. 2005. Survival and condition of big brown bats (*Eptesicus fuscus*) after radiotagging. Journal of Mammalogy 86:95–98.

Ngamprasertwong T., Wangthongchaicharoen M., Racey P. A. 2022. Estimation of roost fidelity of Kitti's hog-nosed bat using mark-recapture approach. Abstract, 19th International Bat Research Conference and 50th Annual Meeting of the North American Society for Bat Research, Austin, TX, USA. 7-12 August 2022.

Norman A. P., Jones G., Arlettaz R. 1999. Noctuid moths show neural and behavioural responses to sounds made by some bat-marking rings. Animal Behaviour 57:829–835.

O'Donnell C. F. J. 2001. Home range and use of space by *Chalinolobus tuberculatus*, a temperate rainforest bat from New Zealand. Journal of Zoology, London 253:253–264.

O'Donnell C. F. J. 2002. Timing of breeding, productivity and survival of long-tailed bats *Chalinolobus tuberculatus* (Chiroptera: Vespertilionidae) in

cold-temperate rainforest in New Zealand. Journal of Zoology, London 257:311–323.

O'Shea T. J., Ellision L. E., Stanley T. R. 2004. Survival estimation in bats: historical overview, critical appraisal, and suggestions for new approaches. In: Thompson W.L., editor. Sampling rare or elusive species: concepts, designs, and techniques for estimating population parameters. Island Press; p. 29–36.

Perry A. E., Beckett G. 1966. Skeletal damage as a result of band injury in bats. Journal of Mammalogy 47:131–132.

PharmaSeq. 2012. White Paper. Tagging of laboratory mice using electronic p-Chips. https://www.isenet.it/wp-content/uploads/2017/01/PharmaSeq_White_Paper_Small_Animal_Tagging.pdf.

Phillips W. R. 1985. The use of bird bands for marking tree-dwelling bats: a preliminary appraisal. Macroderma 1:17–21.

Pierson E. D., Fellers G. M. 1994. Injuries to *Plecotus townsendii* from lipped wing bands. Bat Research News 34:89–91.

Powell R. A., Proulx G. 2003. Trapping and marking terrestrial mammals for research: integrating ethics, performance criteria, techniques, and common sense. Institute for Laboratory Animal Research 44:259–276.

Prentice E. F., Park D. L. 1984. A study to determine the biological feasibility of a new fish tagging system. Annual Report of Research, Bonneville Power Administration and National Marine Fisheries Service, USA.

R Core Team. 2021. R: A language and environment for statistical computing. R Foundation for Statistical Computing, Vienna, Austria. URL https://www.R-project.org/.

Reeder D. M., Kosteczko N. S., Raff H., Kunz T. H., Widmaier E. P. 2006. The hormonal and behavioural response to group formation, seasonal changes and resistant stress in highly social Malayan flying fox (*Pteropus vampyrus*) and the solitary little golden-mantled flying fox (*P. pumilus*) (Chiroptera: Pteropodidae). Hormones and Behaviour 49:484–500.

Rigby E. L., Aegerter J., Brash M., Altringham J. D., 2012. Impact of PIT tagging on recapture rates, body condition and reproductive success of wild Daubenton's bats (*Myotis daubentonii*). Veterinary Record 170:101–101.

Robinson E. J. H., Mandecki W. 2011. Distributed decisions: new insights from radio-tagged ants. In: Sun E.C., editor. Ant colonies: behavior in insects and computer applications. Nova Science Publishers, Inc.; p. 109–128.

Robinson E. J. H., Feinerman O., Franks N. R. 2014. How collective comparisons emerge without individual comparisons of the options. Proceedings of the Royal Society B: Biological Sciences 281: 20140737.

Robinson E. J. H., Richardson T. O., Sendova-Franks A. B., Feinerman O., Franks N. R. 2009. Radiotagging reveals the roles of corpulence, experience and social information in ant decision making. Behavioural Ecology and Sociobiology 63:627–636.

Rybar P. 1973. Remarks on banding and protection of bats. Periodicum Bilogorum 75:177–179.

Satterthwaite F. E. 1946. An approximate distribution of estimates of variance components. Biometrics Bulletin 2:110–114.

Silvy N. J., Lopez, R. R., Peterson, M. J. 2012. Techniques for marking wildlife. In: Silvy NJ, editor. The wildlife techniques manual. The John Hopkins University Press; p. 230–257.

Sikes R. S., and the Animal Care and Use Committee of the American Society of Mammalogists. 2016. 2016 Guidelines of the American Society of Mammalogists for the use of wild mammals in research and education. Journal of Mammalogy 97:663–688.

Skrinyer A. J., Faure P. A., Dannemiller S., Ball H. C., Delaney K. H., Orman R., Stewart M., Cooper L. N. 2017. Care and husbandry of the world's only flying mammals. Laboratory Animal Science Professional 6:24–27.

Smith C. S., Epstein J. H., Breed A. C., Plowright R. K., Olival K. J., de Jong C., Daszak P., Field H. E. 2011. Satellite telemetry and long-range bat movements. Public Library of Science One 6:e14696.

Smyth B., Nebel S. 2013. Passive integrated transponder (PIT) tags in the study of animal movement. Nature Education Knowledge 4:3.

Stebbings R. E. 1978. Marking bats. In: Stonehouse B, editor. Animal marking: recognition marking of animals in research. The Macmillan Press Ltd., London, United Kingdom; p.812–94.

Tenczar P., Lutz C. C., Rao V. D., Goldenfeld N., Robinson G. E. 2014. Automated monitoring reveals extreme interindividual variation and

plasticity in honeybee foraging activity levels. Animal Behaviour 95:41–48.

Trapido H., Crowe P. E. 1946. A wing-banding method in the study of the travel of bats. Journal of Mammalogy 27:224–226.

Vardon M. J., Tidemann C. R. 2000. The black flying-fox (*Pteropus Alecto*) in north Australia: juvenile mortality and longevity. Australian Journal of Zoology 48:91–97.

Voulodimos A. S., Patrikakis C. Z., Sideridis A. B., Ntafis V. A., Xylouri E. M. 2010. A complete farm management system based on animal identification using RFID technology. Computers and Electronics in Agriculture 70:380–388.

Want, R. 2006. An introduction to RFID technology. IEEE Pervasive Computing, 5(1), 25–33.

Wickham, H. 2016. ggplot2: Elegant graphics for data analysis. Springer Nature.

Xu S., Chen M., Feng T., Zhan L., Zhou L., Yu G. 2021. Use ggbreak to effectively utilize plotting space to deal with large datasets and outliers. Frontiers in Genetics 12:774846.

Young R. A. 2001. The eastern horseshoe bat, *Rhinolophus megaphylus*, in southeast Queensland, Australia: colony demography and dynamics, activity levels, seasonal weight changes, and capture-recapture analysis. Wildlife Research 28:425–434.

Zubaid, A., McCracken, G. F., & Kunz, T. H. (eds.). 2006. Functional and Evolutionary Ecology of Bats. Oxford University Press.

Chapter 3 – Using HotSpotter to identify individual big brown bats (*Eptesicus fuscus*) via collagen-elastin bundle patterns

Abstract

Collagen-elastin (CE) bundle patterns in the bat wing membrane have been used to identify individuals (Amelon et al. 2017); however, this method has not been widely adopted, likely owing to the laborious nature of manually comparing images through visual inspection. I tested the effectiveness of using an accessible, feature-based pattern-recognition software—HotSpotter©—to partially automate individual identification using the patterns of CE bundles in bat wing membrane. I created two separate databases of bat wing images from a captive colony of big brown bats (*Eptesicus fuscus*): (1) the *adult database* (n = 192 photos) consisting of 24 adult female bats, and (2) the *juvenile database* (n = 136 photos) consisting of 34 juvenile bats. Photos were taken while illuminating the ventral surface of the wing with ultraviolet (UV) light. Upon running a match comparison (i.e. *query*) on a selected reference image, HotSpotter assigns a similarity score to every other photo in the database and displays the top-ranked images, (n = 6, by default). Query outputs were classified as: (1) positive matches (+Ms), when the top-ranked image was a correct match, (2) negative matches (–Ms), when all 6 top-ranked images were incorrect matches, (3) neutral matches (NMs), when the top-ranked image was incorrect but one of the remaining 5 images was a correct match, or (4) opposite wing matches (OWMs), when an image of the opposite wing was one of the top 6 ranked images. With this method, I found a 60% +M and 17% –M rate for the adult database, whereas the juvenile database had a 27%

+M and 47% –M rate. The +M rate for both databases increased as the number of top-ranked images included when selecting a possible correct match increased. The results demonstrate that pattern-recognition software, like HotSpotter©, has potential to accurately identify individual *E. fuscus* using photos of CE patterns in the wing.

Introduction

Animal identification is critical in addressing many questions regarding wildlife ecology, conservation, and management for various animals. Researchers commonly apply external tags to distinguish animals that lack distinctive features (Silvy et al. 2012). However, external tags may not be permanent plus they can affect behavior, survival potential, and/or cause injury. Biometric markers (i.e. "biomarkers") are an alternative method for animal identification. Biomarkers include characteristic features that are (1) universally shared across all members of a species, (2) distinctive between individuals, (3) permanent over time, and (4) accessible for collection (e.g. being able to photograph or sample) (Jain et al. 2004). Common biomarkers in mammals include unique spots, stripe patterns, DNA, body morphology, fingerprints, and/or characteristic vocalizations.

For bats specifically, there is a wide suite of viable biomarkers including samples from fur, wing membrane, bones, nails, blood, guano, internal organ tissue, teeth, or breath (Brewer et al. 2021). Although these samples provide useful information on an animal's life history, they may not be suitable for individual identification as they are subject to change. Some researchers have used differences in the frequency-modulations of bat calls to distinguish bat species (e.g. Britzke et al. 2011; Murray et al. 2001; O'Farrell and Gannon, 1999); however, bat calls tend to be consistent within a species and therefore unsuitable for individual identification. An interesting case for biometric recognition in bats is for the genus *Balionycteryis* because their patagia are marked with unique spot patterns. Hodgkison et al. (2003) found that spotted-winged fruit bats

(*Balionycteris maculata*) —a bat species known to lack tolerance for external tags— could be distinguished and identified by comparing the number and relative position of spots in their wing membrane. More recently, some Antillean Long-tongued bats (*Monophyllus redmani*) and Insular Single-leaf bats (*M. plethodon*) could be identified from distinctive white patches of fur, visible under ultraviolet (UV) light (Kurta et al. 2023).

A proposed biomarker for bat identification are the bundles of collagen and elastin that are present and easily visible in most if not all bat species (Fig. 3.1; Amelon et al. 2017; Cheney et al. 2017; Church and Warren, 1968). Collagen-elastin (CE) bundles are an essential connective tissue that provide the wing membrane with flexibility and strength, improve the membranes resistance to tearing, allow for the active modulation of wing shape and refinement of aerial agility, and contribute to the wings ability to adapt to changes in aerodynamic forces (Holbrook and Odland, 1978; Swartz and Allen, 2020; Timpe et al. 2013; Vaughn, 1970). The CE bundles also provide a wrinkly texture to the wing membrane (Holbrook and Odland, 1978). It is believed that CE bundles help maintain tension in wing membrane, keep the membrane taut during flight, and counter flutter behaviours (Cheney et al 2015; Swartz et al. 1996; Timpe et al 2013; Vaughn 1996). The CE bundles are typically oriented in the mediolateral direction along the axis spanning the wing (Swartz & Allen, 2020); however, this general pattern varies between bat species and families, especially in the following areas: (1) adjacent to the skeleton of the digits, (2) around the midpoint

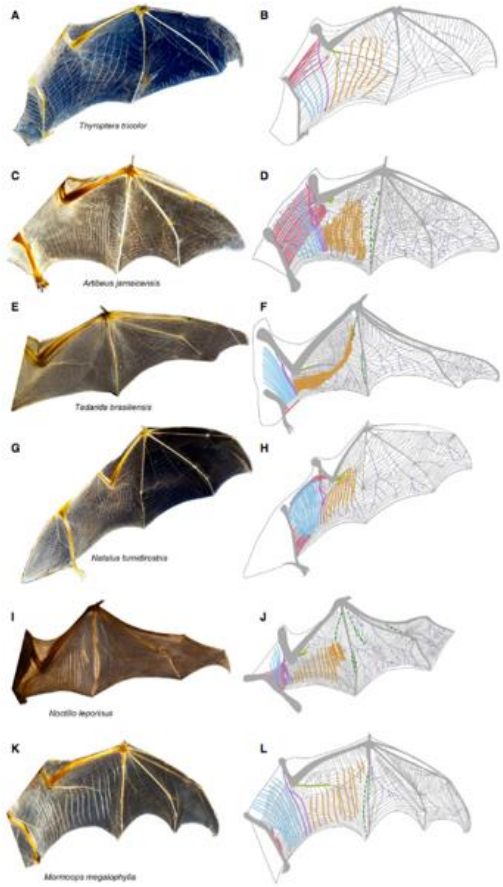

Fig. 3.1.—Diversity in wing membrane architecture. Cross-polarized light images and schematics showing elastin bundles (grey lines), muscle arrays (solid colored lines), neurovasculature (dashed blue lines), and collagenous fiber bundles (dashed green lines). Schematics were developed using multiple cross-polarized light images. Muscle arrays are tibiopatagiales (red), dorsopatagiales (blue), corcacopatagiales (purple), plagiopatagiales proprii (orange), cubitopatagiales (green). Familes: (A,B) Thyropteridae; (C,D) Phyllostomidae; (E,F) Molossidae; (G,H) Natalidae; (I,J) Noctilionidae; (K,L) Mormoopidae. Image shown taken from Fig. 4. of Cheney et al. (2017).

between the V and VI metacarpal and (3) in the rostrodistal plagiopatagium, between the forearm and fifth metacarpal, rostral to the plagiogatgiales proprii (Fig. 3.1; Cheney et al. 2017). Visual inspection of CE bundle patterns is known to be an effective strategy to distinguish some bat species, even if part of the wing membrane is damaged (Amelon et al. 2017). However, this technique has yet to be adopted, likely due to the laborious nature of manually evaluating images of wings through visual inspection.

We recommend using pattern-recognition software to help alleviate the manual labour associated with visual inspection and to automate the process of evaluating CE bundles for bat identification. Different types of pattern-recognition software can be broadly distinguished into pixel-based programs (PBPs) or feature-based programs (FBPs) (Matthé et al. 2017). The PBPs compare pixels of a reference image to pixels in a test image at identical spatial locations (Fig. 3.2). Therefore, PBPs are extremely sensitive to photo orientation, quality, resolution and size. Conversely, FBPs use regions of interest (ROIs) to compare detectable features (e.g., spots, stripes, etc.) between a reference image and test images (Fig. 3.2).

HotSpotter© (Crall et al. 2013) is a free-to-use, FBP that implements a 2-algorithm approach for comparing reference and test images (i.e. a *query*). First, HotSpotter utilizes a Scale Invariant Feature Transform (SIFT) algorithm (Lowe, 2004) to define features in a given ROI (i.e. a “chip”). The SIFT algorithm is used for one-to-one image comparisons and determines matches in features despite variance in scale, illumination, and orientation between photos. HotSpotter uses a

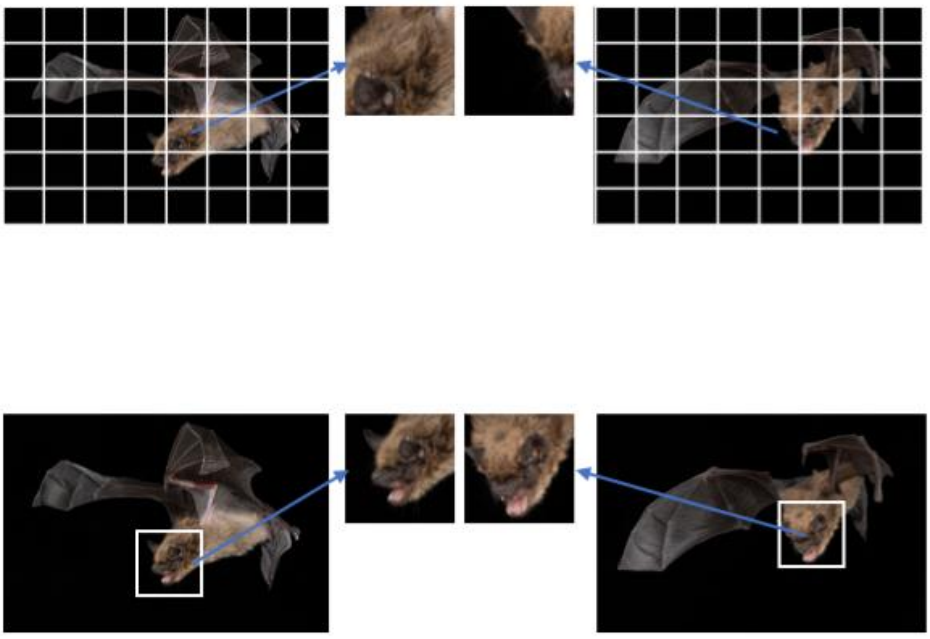

Fig. 3.2.—Visual depiction of two categories of pattern-recognition software: (A) Pixel-based programs (PBPs). PBPs utilize the pixel composition in each photo being tested and evaluate pixel intensity. Pixels of identical spatial location are compared between test and reference images, making PBPs sensitive to photo orientation, quality, resolution and size. **(B) Feature-based program (FBPs).** FBPs utilize detectable features within a predefined region of interest (ROI). Features could include spots, stripes, finger prints, or any detectable patterns / changes in illumination between photos. The features within the ROIs are then compared between reference and test images. HotSpotter is an FBP.

Local Naïve Bayes Nearest Neighbour (LNBNN) algorithm (McCann and Lowe, 2012) to perform one-vs-many comparisons within a defined database of images. Each feature in the queried chip (i.e. *qcid*) that HotSpotter matches to a feature in a test image chip (i.e. *cid*) is given a similarity weighting based on results from both the SIFT and LNBNN algorithms. These weighted similarities are then summated into a total similarity score: a larger score indicates a stronger similarity between the *qcid* and *cids*. A thorough HotSpotter User Guide describes the installation (Download Link: https://github.com/Erotemic/ hotspotter) and HotSpotter use on Windows, MacOS, and/or Linux (Crall et al. 2013). To date, HotSpotter has been successful in identifying and distinguishing many animals including zebras (Berger-Wolf et al. 2016; Lea et al. 2018), jaguars (Smyth et al. 2022), leopards (Park et al. 2019), margays (Harmsen et al. 2021), giraffes (Crall et al. 2013), lionfish (Crall et al. 2013), toads (Burgstaller et al. 2021), frogs (Patel and Das 2020; Duhé 2018), ocelots (Nipko et al. 2020), beetles (Quinby et al. 2021), tigers (Cheema et al. 2017), seals (Nepoyinnykh et al. 2023; Vilkman, 2022), sea turtles (Dunbar et al. 2021; Hanna et al. 2021; Tabuki et al. 2021), snow leopards (Bohnett et al. 2023; Blount et al. 2022; Miguel et al. 2019), snakes (Olsen 2023), and whales (Cheeseman et al. 2022; Khan et al. 2022).

The purpose of this study was to determine if HotSpotter is able to identify bats through examination of CE bundle patterns. To evaluate the efficacy of HotSpotter, we compared photos of wing membranes in big brown bats (*Eptesicus fuscus*) from a captive colony. Since the photos were of bats with known identities, we assessed if HotSpotter was able to correctly match photos of the

same animal. Since pregnant *E. fuscus* in western populations typically give birth to twins in a birthing cycle (Christian 1956; Hood et al. 2002; Kurta and Baker, 1990), we assessed if HotSpotter could match known sibling pup pairings.

Materials & Methods

Animals – We collected photos from adult female big brown bats (*Eptesicus fuscus*; n = 24) and their offspring (n = 34) from a captive colony at McMaster University. Prior to this study, each adult bat received both a single passive integrated transponder (PIT) tag injected subcutaneously in the back between the shoulder blades, and a coloured, numbered plastic split-ring band on their forearm for individual identification. To distinguish pups, we routinely applied toe nail paint until they were of sufficient weight and age to apply a plastic split-ring band and PIT tag. Roughly equal numbers of female (n = 19) and male (n = 15) pups were tested. All bats were monitored for health changes during the study. These experimental procedures were approved by the Animal Research Ethics Board of McMaster University and adhered to the Guide to the Care and Use of Experimental Animals published by the Canadian Council of Animal Care. Bats were housed in a husbandry facility where the temperature and lighting varied seasonally, following the ambient pattern. The facility consisted of two indoor ($2.5 \times 1.5 \times 2.3$ m; l × w × h) areas, one of which was connected through a hole in the wall, to a larger outdoor area ($2.5 \times 3.8 \times 2.7$ m; l × w × h) that free-flying bats were permitted to access. Food (mealworms; *Tenebrio molitor*) and water were provided *ad libitum*.

Photograph Collection & HotSpotter Use – We collected 192 wing photos from 24 adult female big brown bats (*Eptesicus fuscus*) over the course of 40 days (Table 3.1). Equal number wing photos were taken for each bat (n = 4 per wing per adult bat) for both the left and right wing membranes (n = 96 each). We collected one photo per wing of a bat on any given recording day and photos of the same bat were taken on staggered days, with some separation (range = 5–20 days) (Table 3.1). We also collected 136 wing photos from 34 *E. fuscus* pups when they were between post-natal day (PND) 39 – 54 (n = 2 per wing per pup) (Table 3.2). The rear-facing camera of an iPhone 11 was used to take images. The iPhone 11 camera has Dual 12MP six-element wide lens (f/1.8 aperture) and five-element ultra-wide (f/2.4 aperture) camera lens, auto optical image stabilization, sapphire crystal lens cover, night mode, 2x optical and 5x digital zoom, and 100% focus pixels. Each photo was taken in a dark room, where we outstretched the wing of the bat over a black-felt draped over a table and illuminated the ventral surface of the wing membrane with an ultraviolet (UV) flashlight (DarkBeam®, wavelength = 365 nm). We manipulated the angle of the UV flashlight for each photo in attempt to emphasize the CE bundle pattern. We also ensured that the whole wing membrane (i.e., both the plagiopatagium and dactylopatagium) was captured and that each image was oriented correctly with the radius & ulna at the top (Fig. 3.3). We cropped photos as needed to ensure most of the image space consisted of the wing membrane.

We imported all of the photos into two separate HotSpotter databases: (1) the *adult database* consisted of all adult photos (n = 192) and, (2) the *juvenile*

Table. 3.1. –Data Collection Days for left and right wing membrane photos of adult, female big brown bats.

Bat ID	31 May	02 June	07 June	08 June	12 June	14 June	19 June	21 June	23 June	27 June	29 June	04 July	06 July	10 July
Sky 101	X			X		X					X			
Sky 103	X			X		X					X			
Sky 104			X		X				X				X	
Sky 106			X		X				X				X	
Sky 107	X			X		X					X			
Sky 108				X		X					X			X
Sky 109			X		X				X				X	
Sky 110	X			X		X						X		
Sky 111	X			X		X						X		
Sky 112	X			X				X				X		
Sky 113	X			X		X						X		
Sky 114		X		X				X					X	
Sky 115			X		X				X				X	
Sky 116		X		X				X					X	
Sky 117		X		X						X				X
Sky 118		X		X						X				X
Sky 119		X		X						X				X
Sky 120			X		X				X				X	
Sky 121		X		X						X				X
Sky 123		X		X						X				X
Sky 124			X		X						X			X
Sky 125			X		X		X						X	
Sky 126			X		X		X						X	
Sky 127				X				X			X			X

Note: An " X" denotes a day where photos of the bat' s left and ring were collected

Table. 3.2. –Data Collection Days for left and right wing membrane photos of juvenile big brown bats, *Eptesicus fuscus*.

Mom ID	Pup ID (Sex)	Date of Birth	27 July	28 July	31 July	01 Aug	03 Aug	08 Aug	09 Aug
Sky 101	G120 (M)	16 June	X			X			
Sky 103	G195 (F)	16 June	X						X
	G196 (F)	16 June	X			X			
Sky 104	G115 (M)	19 June			X		X		
	G228 (F)	19 June			X			X	
Sky 106	G222 (M)	19 June				X			X
	G223 (M)	19 June			X			X	
Sky 107	G108 (M)	18 June		X			X		
Sky 108	G229 (F)	19 June			X			X	
	G230 (M)	19 June				X			X
Sky 109	G231 (M)	19 June			X			X	
	G232 (F)	19 June			X			X	
Sky 110	G118 (F)	17 June	X			X			
	G119 (F)	17 June	X				X		
Sky 111	G112 (M)	17 June	X				X		
	G113 (F)	17 June	X				X		
Sky 112	G193 (F)	14 June	X			X			
	G194 (M)	14 June	X			X			
Sky 113	G116 (M)	17 June		X			X		
	G117 (F)	17 June		X			X		
Sky 114	G221 (F)	18 June		X			X		
Sky 115	G233 (M)	22 June			X			X	
	G234 (M)	22 June			X			X	
Sky 116	G124 (F)	19 June			X		X		
Sky 117	G197 (F)	18 June		X			X		
	G198 (M)	18 June		X			X		
Sky 118	G191 (F)	16 June	X			X			
	G192 (F)	16 June	X			X			
Sky 119	G199 (M)	18 June		X			X		
	G200 (F)	18 June		X			X		
Sky 123	G235 (F)	21 June			X			X	
	G236 (M)	21 June			X				X
Sky 124	G226 (F)	18 June			X			X	
	G227 (F)	18 June		X				X	

Note: An “X” denotes a day where photos of the bat’s left and ring were taken. “M” represents Male and “F represents Female. All pups were born in 2023.

database one consisting of all pup photos (n = 136). For every image, a ROI was manually generated using a built-in feature that allows the user to define a chip (rectangular area) for a given image by clicking two diagonal corners. To standardize photo orientation and chip selection, we flipped left wing images 180º along the x-axis so that the wing orientation was consistent across all photos. The first selected point was always near the bottom of the wing, caudal to the bat and the second point was always near the distal portion of the wing near the tip. We were able to redefine chip orientation and size in HotSpotter, if necessary. For convenience, users may also convert whole images into chips. We then input a Chip ID —the bat's band ID (e.g. Sky 111)— as an identifier for the chip. HotSpotter then computed features within the ROI (*orange dots*; Fig. 3.3) which represent scale extrema of a Hessian-Hessian operator (Perd'och et al. 2009) and each feature is fit with an orientation elliptical (Mikolajczyk et al. 2005).

To conduct image comparisons in HotSpotter, users must run a *query* on a reference chip which will implement the SIFT and LNBNN processes for feature comparison. After conducting a query, HotSpotter displays the queried chip (*qcid*) on top of another chip from a test image (*cid*) with weighted lines highlighting similar features detected between the two chips (Fig. 3.4). The color of the weighted lines represent the strength of similarity between the features across chips and the similarity score represents a summation of the weight values attributed to each of the weighted lines (Fig. 3.4). By default, HotSpotter compares and ranks the *qcid* to all other chips in the database —based on similarity score— but only displays the 6 top-ranked images. By using Chip IDs,

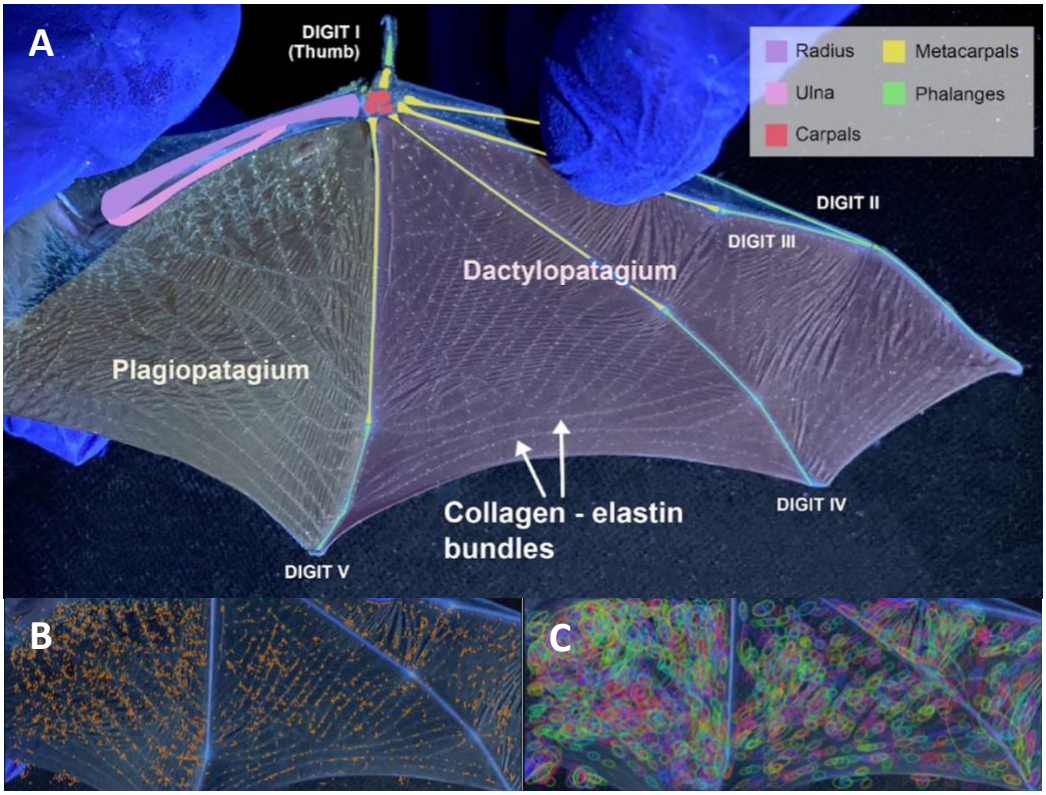

Fig. 3.3. —Representative photograph of a bat's left wing with: (A) labeled anatomy. The plagiopatagium (shaded light yellow) makes contact with the radius (purple), the ulna (pink) and the dactylopatagium (shaded light purple). The yellow lines represent the metacarpals, numbered in relation to the digits of the wing (I–V). Metacarpals radiate from the carpals (red). Phalanges extend from the ends of metacarpals (green), forming the digits of the wing. **(B) detected features.** Features are detected within HotSpotter and depicted as orange dots within the images ROI (i.e. chip). Note, features can be detected anywhere on the image, but appear to follow collagen-elastin bundle patterns closely. **(C) Orientation ellipticals.** Each orientation elliptical is fit to a single, detected feature and create a spatial map of each feature. The photo is of the left wing of SKY125 (Photo Number: 6729).

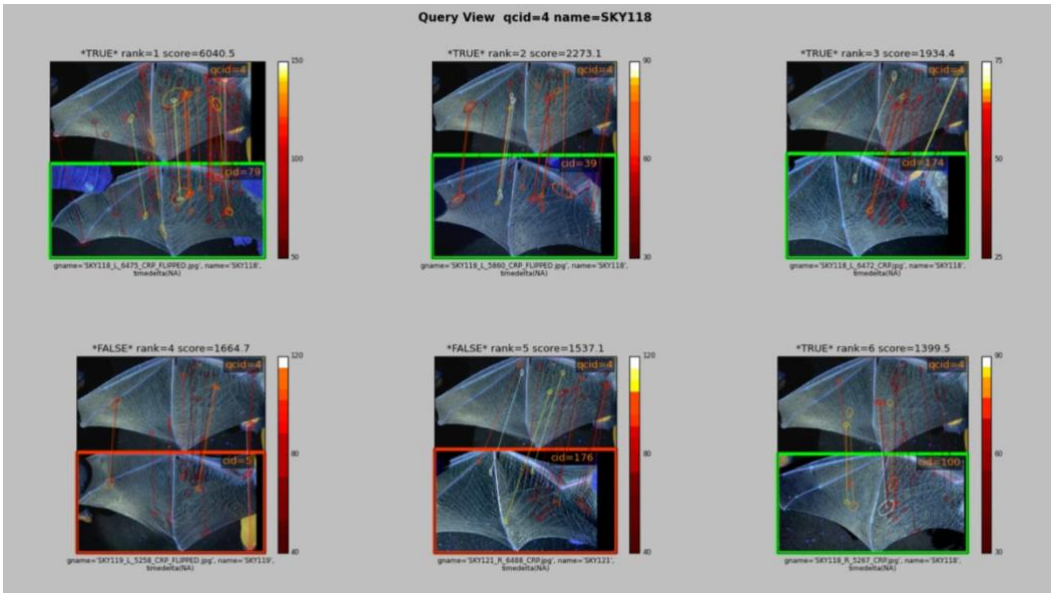

Fig. 3.4.—Representative output from a HotSpotter Query. The six panels represent the 6 top-ranked test images (bottom; *cid*) compared to the queried image (top; *qcid*). Images are ranked by similarity scores. Lines between images represent weighted similarity lines and are assigned colors from dark-red to yellow/white based on increasing strength of similarity score (ranges differ between *cids*, scales are to the right of each photo pair). Green boxes around *cids* represent correct matches and red boxes represent incorrect matches. Note, this query output represents both a +M (the 3 top-ranked images are correct matches) and an OWM (the 6th ranked image is of the same animal, opposite wing)

HotSpotter can denote whether two matched chips were of the same animal (*Correct Match*), or of different animals (*Incorrect Match*). We classified each output as either a *Positive Match* (+M), *Negative Match* (–M), *Neutral Match* (NM), or an *Opposite Wing Match* (OWM). A +M denotes that the top-ranked image was a correct match whereas a –M denotes that there were no correct matches within the 6 top-ranked images. An NM represents an occurrence where the top-ranked image was not a correct match, but a correct match appeared somewhere else in 6 top-ranked images. Therefore, the summation of +Ms and NMs displays all occurrences of a correct match within the 6 top-ranked images. An OWM represents the occurrence of a correct match of the bat's opposite wing. For pup photos, we also examined instances of *Positive Sibling Matches* (+SMs) and *Opposite Wing, Sibling Matches* (OWSMs): A +SM occurs when one of the 6 top-ranked images was of the same wing in the sibling of the pup in the queried image whereas an OWSM is when one of the 6 top-ranked images was of the opposite wing in the sibling. We evaluated the proportions of each match type for all query results in the adult and juvenile databases separately. Since we found no significant differences in proportions for any match type between left and right wing photos, we report pooled summary data for each database.

Data Analyses – Data analysis was conducted in R (R Core Team, 2021) and data were visualized with the *ggplot2* (Wickham et al. 2016) and *plotrix* (Lemon, 2006) packages. Unless stated otherwise, summary data are displayed as the mean ($\bar{X}$) ± standard error (*SE*), with applicable measures reported with 95% confidence intervals (CI). We used the plus 4 method (Agresti and Coull, 1998) in

R to calculate 95% confidence intervals for proportions. We tested whether there were significant differences ($\alpha = 0.05$) between proportions using the *prop.test* function in R (Baldi and Moore, 2014). We conducted Analysis of Variance (ANOVA) tests to evaluate the main effect of Rank (from 1–6), Match (Correct, Incorrect, and Opposite Wing), and the Rank × Match interaction on similarity scores. For these analyses, we fit each model to the data using the *lmer* function, included BatID as a random effect, and calculated the degrees of freedom using Satterthwaite's method (Satterthwaite, 1946). Tukey Honestly Significant Difference (i.e. Tukey HSD) *post-hoc* analyses were conducted to evaluate pairwise differences between both distributions of similarity scores and proportions. For pairwise comparisons between proportions, p-values were adjusted using the Holm-Bonferroni method. Note, variables with different letters (*a–d*) are significantly different through the results of Tukey HSD tests.

Results

Similarity Scores – A metric that can be used to determine the likeliness of a correct match are the similarity scores HotSpotter assigns between *qcids* and *cids*. We recorded similarity scores for the 6 top-ranked images after running individual queries on all images in the adult (n = 192 photos) and juvenile databases (n = 136 photos), separately. The similarity scores tended to be quite variable for both the adult ($\bar{X} \pm SD$ = 1996.3 ± 1032.9; range = 492.6–9961) and juvenile database (1862.4 ± 873.3; range = 500.8–8505.4). Note, similarity scores are influenced by sample size and the species being evaluated (Crall et al. 2013).

We found a significant main effect of Rank ($F_{5,1118} = 29.46$, $P < 0.001$), Match ($F_{2,1123} = 7.68$, $P < 0.001$), and Rank × Match interaction ($F_{10,1119} = 3.47$, $P < 0.001$), for the adult database. Similarly, we found a significant main effect of Rank ($F_{5,765} = 15.04$, $P < 0.001$), Match ($F_{4,767} = 2.39$, $P = 0.05$) and Rank × Match interaction ($F_{18,766} = 2.10$, $P < 0.001$) for the juvenile database. In the adult database, a follow up analysis examining the effect of Rank separately for each Match found a significant effect of Rank for Correct Matches ($F_{5,235} = 24.79$, $P < 0.001$), Incorrect Matches ($F_{5,851} = 49.98$, $P < 0.001$), and Opposite Wing Matches ($F_{5,20} = 3.14$, $P = 0.03$). Conversely, the effect of Rank was significant for Opposite Wing Matches ($F_{5,14} = 4.64$, $P = 0.01$), and Incorrect ($F_{5,661} = 31.34$, $P < 0.001$) for the juvenile database, but not significant for Correct ($F_{5,43} = 1.74$, $P = 0.15$), Sibling Correct ($F_{5,29} = 1.91$, $P = 0.12$), or Opposite Wing Sibling Matches ($F_{3,2} = 13.44$, $P = 0.07$).

We then conducted *post hoc* Tukey HSD tests to evaluate pairwise comparisons of similarity scores for each Rank. For both databases, similarity scores tended to decrease as Rank increases (Fig. 3.5). In the adult database, Rank 1 (*a*) and Rank 2 (*b*) similarity scores differed significantly from each other and the other ranks. Rank 3 (*c*) similarity scores also differed significantly from Rank 5 (*d*) and Rank 6 (*d*) similarity scores, but not from Rank 4 (*cd*) similarity scores (Fig. 3.5). Results from the juvenile database data showed a similar trend: Rank 1 (*a*) and Rank 2 (*b*) similarity scores differed significantly, but Rank 2 (*b*) and Rank 3 (*bc*) similarity scores did not significantly differ, nor did Rank 3 (*bc*) from Rank 4 (*cd*) or Rank 5 (*cd*) (Fig. 3.5). We also evaluated pairwise comparisons for

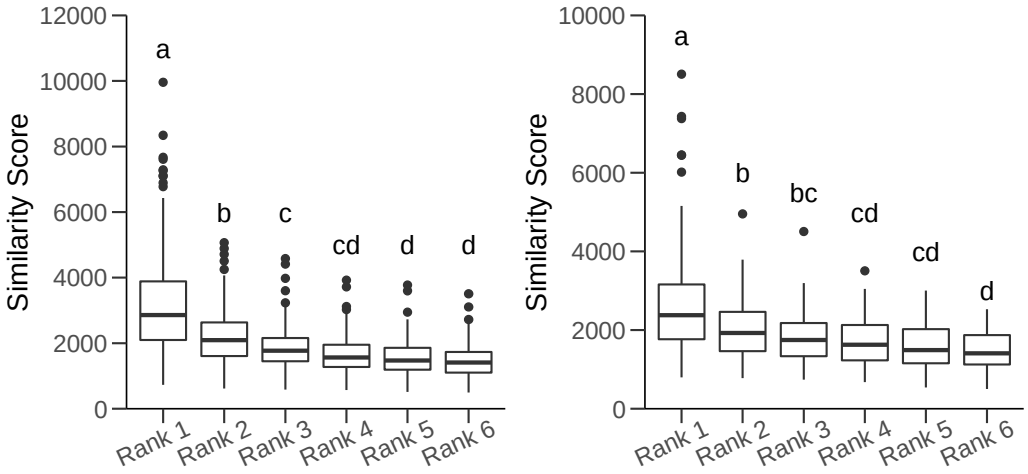

Fig. 3.5.—Distribution of similarity scores across the 6 top-ranked images. Data show the median (*bolded line*), 25th and 75th percentiles (*top and bottom of each box*), 10th and 90th percentiles (*bars*) and outliers (*black dots*) for similarity scores in the adult (*left panel*) and juvenile databases (*right panel*). Similarity scores are computed by HotSpotter by running queries of images within the database. Note, HotSpotter intrinsically ranks images based on similarity score, so we would expect similarity score to increase as rank number increases. Letters (*a*–*d*) indicate the results of Tukey HSD pairwise comparison tests.

similarity scores between matches using *post hoc* Tukey HSD tests. Correct matches of the same wing (*a*) had significantly greater similarity scores compared to correct matches of the opposite wing (*b*) and incorrect matches (*b*) for the adult database (Fig. 3.6). Similarly, correct matches (*a*) were significantly greater than all other matches evaluated for the juvenile database, including matches of the opposite wing (*b*), incorrect matches (*b*), matches of the same wing in the animals sibling (*b*), and matches of the siblings opposite wing (*b*) (Fig. 3.6).

Proportions of Match Types – We calculated the proportions of +Ms, –Ms, NMs and OWMs for the two databases separately (Fig. 3.7). We found a significant difference in proportions for the adult ($X^2 = 129.87$, $d.f. = 3$, $P < 0.001$) and juvenile database ($X^2 = 36.17$, $d.f. = 3$, $P < 0.001$). Using *post hoc* Tukey HSD analyses, we found that the proportion of +Ms was significantly larger than all other match types for the adult database. Conversely, the proportion of –Ms was significantly larger than all other match types for the juvenile database and the difference between +Ms and OWMs approached significance ($P = 0.05$) (Fig. 3.7). We also evaluated occurrences where a test image of a pups sibling, either of the same wing (+SM) or of the opposite wing (OWSM) appeared in the 6 top-ranked images for the juvenile database (Fig. 3.7). By definition, the sum of +Ms and NMs will provide the proportion where a correct match occurs in the 6 top-ranked images (0.51) whereas taking the summed proportion of +SMs and OWSMs will give the proportion where a correct match of the animals sibling occurred (0.30): these proportions were significantly different ($X^2 = 11.93$, $d.f. =$

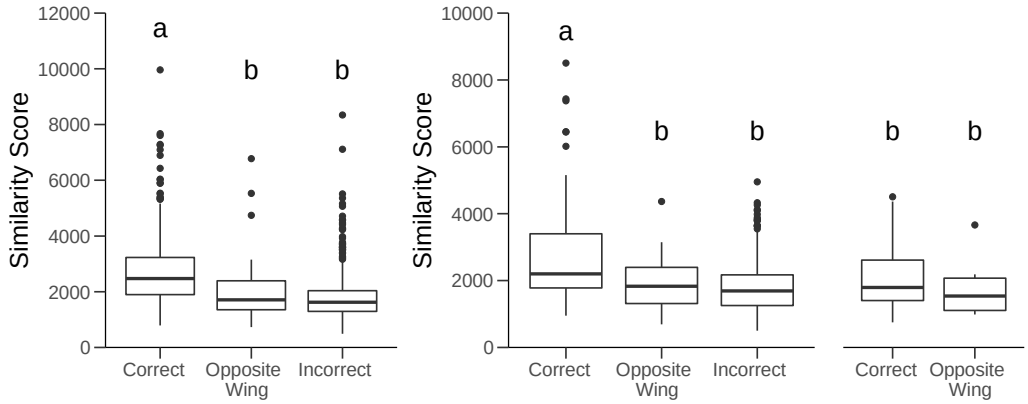

Fig. 3.6.—Distribution of similarity scores for correct, opposite wing, and incorrect matches. Data illustrate the median (*bolded line*), 25th and 75th percentiles (*top and bottom of each box*), 10th and 90th percentiles (*bars*) and outliers (*black dots*) of similarity scores for different matches regardless of Rank for the adult (*left panel*) and juvenile database (*right panel*). The juvenile database is broken down to same animal (*left portion*) and sibling matches (*right portion*) Similarity scores are computed by HotSpotter by running queries of images within the database. Correct Matches are query matches of the same wing in the same animal. Opposite Wing Matches are query matches of the opposite wing in the same animal. Incorrect Matches are query matches where the reference image and test image are of different animals. Letters (*a*–*d*) indicate the results of Tukey HSD pairwise comparison tests.

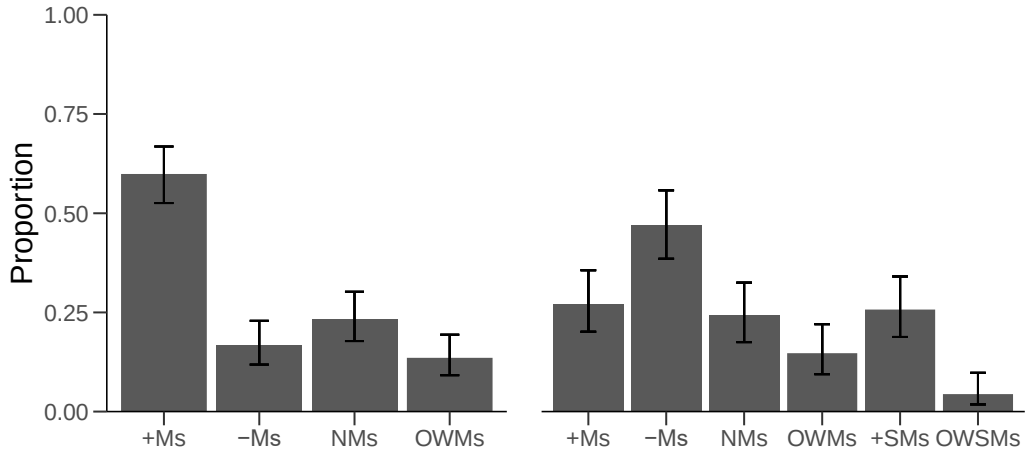

Fig. 3.7.—Proportions for various match types. Data illustrate the proportion of *Positive Matches* (+Ms) *Negative Matches* (–Ms) *Neutral Matches* (NMs) and *Opposite Wing Matches* (OWMs) for both the adult (left) and juvenile (right) database. *Positive Sibling Matches* (+SMs) and *Opposite Wing*, *Sibling Matches* (OWSMs) are included for the juvenile database. Error bars represent 95% CIs calculated using the plus 4 method in R (Agresti and Coull, 1998). See *Materials and Methods* for definitions of each type of match.

1, $P < 0.01$) for the juvenile database. We examined whether twin pairings, either same sex (M/M or F/F) or different sex (F/M), influenced the proportion of sibling matches. The proportions for M/M (0.31), F/F (0.34), and M/F (0.35) were not significantly different ($X^2 = 0.07$, *d.f.* = 2, $P = 0.97$).

The proportion of correct matches increased significantly from 0.60 to 0.73 (95% CI [0.66 – 0.79]) in the adult database, when considering both of the 2 top-ranked images ($X^2 = 6.72$, *d.f.* = 1, $P = 0.01$) (Fig. 3.8) and continued to increase when including more ranks: nearly all queries (~0.97; 95% CI [0.94–0.99]) contain a correct match within the 25 top-ranked images (Fig. 3.8). The proportion of correct matches also increases when you include more top-ranked images in the juvenile database and reaches 0.88 (95% CI [0.81 – 0.93]) within the 50 top-ranked images (Fig. 3.8). We modelled chance probability of these trajectories for both the adult (Equation 1) and juvenile (Equation 2) databases:

$$P_{Correct\ Match}(x) = \frac{{}_{191}C_r - {}_{184}C_r}{{}_{191}C_r} \quad (1)$$

$$P_{Correct\ Match}(x) = \frac{{}_{135}C_r - {}_{132}C_r}{{}_{135}C_r} \quad (2)$$

We used the nCr formula, where *n* represents the total number of photos and *r* represents the number of photos selected from the total sample in the database.

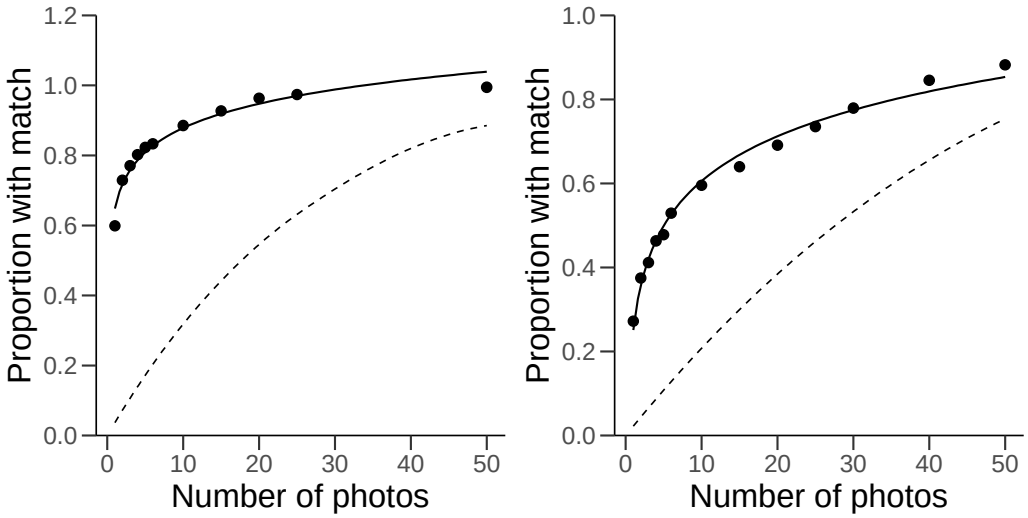

Fig. 3.8.— Cumulative Correct Match Proportion. Data represent proportion of total queries containing a correct match as a function of how many top-ranked photos are included for the adult (*left panel*) and juvenile database (*right panel*). The *dotted lines* represent modelled probabilities (*See* Equation 1 and Equation 2) of obtaining a correct match when selecting a subset of *x* photos. Grey shaded region represents the 95% CI for the fitted lines (*solid lines*).

Discussion

Overall, our results suggest that HotSpotter is a viable method for bat identification. We found that HotSpotter was able to accurately and reliably detect features in the wing membrane (Fig. 3.6) and correctly match photos of big brown bats (*Eptesicus fuscus*) using CE bundle patterns (Fig. 3.7) above chance probability (Fig. 3.8). We found significant main effects of Rank, Match (i.e. correct, incorrect, and opposite wing matches), and Rank × Match interactions for both databases. It was unsurprising to see a main effect of Rank as HotSpotter intrinsically ranks images based on similarity scores; however, it was interesting to see a significant effect of Match and Rank × Match interaction, suggesting that similarity scores are typically higher for correct matches and that correct matches tend to be ranked higher compared to other matches. In other words, HotSpotter reliably assigns high similarity scores to photos of the same individual.

The proportion of +Ms in the adult database (0.60) was significantly larger compared to all other matches (Fig. 3.7). Although this proportion is reduced compared to visual inspection in bats (0.96 Success Rate; Amelon et al. 2017), HotSpotter alleviates the labour of evaluating large datasets of images by filtering photos from a database into a smaller subset needed for visual inspection. Our results show that a correct match is present within the 50 top-ranked images for >80% of all queries, despite differences in sample size or the probability of achieving a successful match (Fig. 3.8). Therefore, our definition of a +M may be diminishing HotSpotter's capabilities: by considering a range of top-ranked images as opposed to accepting the top-ranked image, the success rate can be

increased. HotSpotter effectively reduces the number of images needed to be assessed through visual inspection while minimizing the false error rate. Since the +M is less than 100%, visual examination and subjective choice must always be required when using HotSpotter to identify bats (Gaston and O'Neill 2004).

Wing Symmetry – Our results showed no significant differences in proportions between left and right wing photos, suggesting photos of either wing could be used. We found that similarity scores were significantly higher for +Ms compared to OWMs for both databases, suggesting HotSpotter detects same-wing photos more effectively compared to opposite-wing photos of the same bat. We speculate that there may be a lack of symmetry between left and right wing CE patterns. The proportion of +Ms was significantly larger compared to the proportion of OWMs in both databases, despite the probability of achieving a +M being lower than the probability of OWMs. Similar to other marking methods, we urge researchers to standardize how photographs are taken. To maximize the richness of the database and the likelihood of achieving a correct match, we suggest taking photos of both the left and right wing membranes and including them in a single database (Matthé et al, 2017). In our protocol, we flipped left wing images 180º to ensure all photos were oriented the same way; however, we did not test whether flipping right wing images instead would have changed similarity scores, and/or quantify whether similarity scores or the proportion of +Ms changed as a result of this manipulation.

Injury – We did not manipulate the bat's wing membranes to introduce scar tissue, holes or reduce surface area in our experiment. Overstretching CE

bundles during a biopsy may increase wound size (Faure et al. 2009; Gosline et al. 2002), wound healing times (Greville et al. 2018), and/or alter how the CE patterns regrow during cell proliferation and remodelling (Guo and DiPietro, 2010; Ceballos-Vasquez et al. 2014b). To our knowledge, it is unknown whether CE bundles grow back in similar patterns during wound healing, which could impact the effectiveness of using CE as a biomarker (Jain et al 2004). Moreover, HotSpotter uses all detected features within a chip when running a query including scar tissue, wing tears, or a visible network of dilated blood vessels. Unlike CE bundles, blood vessels may change in location, especially if the wing membrane is injured. Transillumination using white-light can emphasize blood vessel networks (Lollar & Schmidt-French, 2002), whereas UV light emphasizes CE bundles (Amelon et al. 2017). We speculate that wing membrane injuries may not affect the capability of HotSpotter to identify bats as Amelon et al. (2017) found visual inspection was possible even if there was a ≤50% plagiopatagium loss. We urge researchers to assess how naturally induced and/or controlled injury (e.g. wing biopsies) affect CE bundle pattern regrowth.

Juvenile Identification – A secondary purpose of this experiment was to examine CE bundle patterns in bats of known age and sibling pairs. We collected photos from pups between PND 39 – 54 and found the +M rate exceeded the expected probability (Fig. 3.8), albeit the proportion of +Ms was much lower compared to the adult database (Fig. 3.7), likely owing to the reduced probability of achieving a +M and increased probability of achieving a –M compared to the adult database. The age range of pups we recorded from encompasses the

developmental stage where mass and forearm length of pups is expected to be similar to or slightly higher than wild-caught adult *E. fuscus* (PND 45), but is well beyond when bat pups are expected to make flight attempts (PND 7/8), begin exercising wing muscles (PND 13), perform controlled falls (PND 21) or achieve powered flight (PND 27/28) (O'Farrell and Studier, 1973; Buchlear 1980; Moss et al. 1997; Mayberry and Faure, 2014). While piloting this study, we photographed a pup (White 243) at PND 15, who was exhibiting flapping behaviours at the time of photo collection (Fig. 3.9). Interestingly, the CE bundles are somewhat visible in the plagiopatagium, but not in the dactylopatagium (Fig. 3.9). We also noticed that White243's metacarpals were not fully developed at PND 15. This prompted us to record from older pups as: (1) it would be unlikely to encounter or apply external marks to pups this young in the field and (2) it ensures CE patterns were visible. We observed no differences in the proportions of OWMs for different twin pairings (F/F, M/F, or M/M), suggesting there is no sexual dimorphism in CE bundle patterns and that siblings may exhibit similar pattern characteristics.

Correct Match Rate & Influencers – Although we attempted to emphasize the CE bundle patterns by illuminating the ventral surface of the wing membrane with UV light, we cannot rule out that HotSpotter used other features within ROIs during queries. During our pilot study, we noticed HotSpotter incorporated features outside of the wing membrane (e.g. textures of leather glove) that influenced feature detection and resultant similarity scores. Thus, we created ROIs to decrease the signal-to-noise ratio; however, this may have introduced variability as there is likely different sized ROIs across images. We posit that a

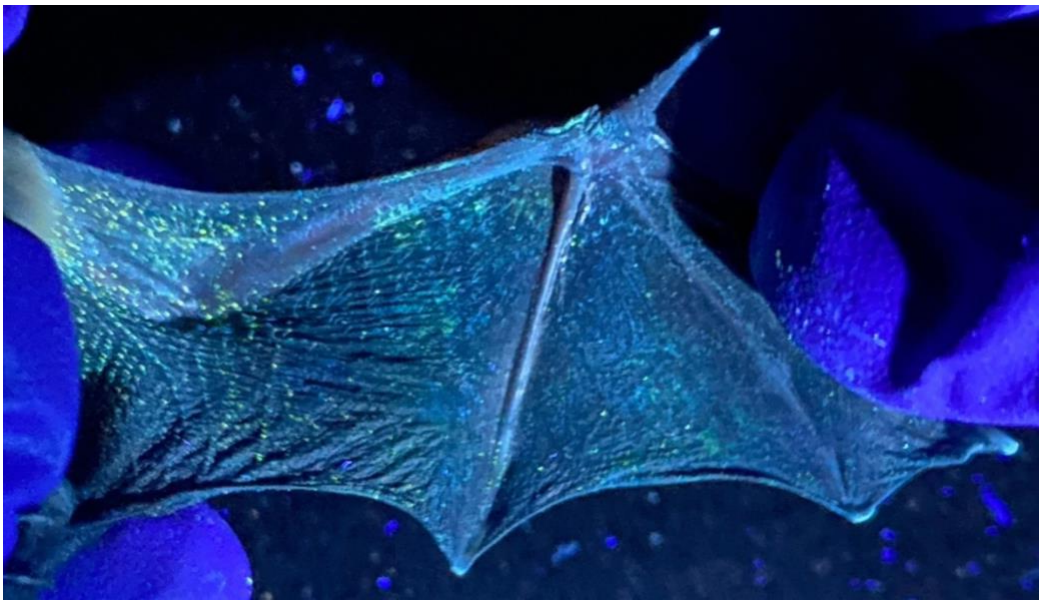

Fig. 3.9. —Photograph of White243 taken at PND 15. Photograph was taken outside of the experiment, serving as pilot data.

lack of photo standardization may be unavoidable as bat restraint and the extension of the wing would be difficult to keep consistent. In our attempt to standardize photo collection, we ensured the wing of the bat was parallel to a flat surface. The UV light was always fixated directly above the bats wing, but the angle of the light was adjusted until the CE bundles were visually emphasized. The angle of the light was influenced by (1) which wing was being photographed, (2) whether the edges of the wing membrane were folded up, creating shadows, and (3) the variation in CE patterns between bats. It is crucial that bats are handled properly to minimize animal stress. We held bat wings by the wrist to avoid damaging wing membrane muscles, tendons and/or bones, which often resulted in the handlers thumb covering some of the wing membrane. Bats should ideally be immobile during photo collection because blurry photos or photos with parts of the wing membrane covered / partially curled may reduce the +M success rate (e.g. Nipko et al. 2020). Since animal handling is required, it is safe to assert that handling experience is required. The captive animals in our study typically remained calm during handling and photo collection. Researchers may consider implementing a device to restrain bats (e.g. Ceballos-Vasquez et al. 2014a) to help standardize the process of wing extension and photo collection. However, the plexiglass may produce reflected light, especially if using transillumination.

Initially, we attempted to use a different wavelength of UV light (395 nm) and found that the contrast in illumination between the CE pattern and the wing membrane was not strong enough for HotSpotter to accurately detect features. We also used an iPhone 11 camera for photography, our rationale being that using a

phone camera is considerably more accessible compared to purchasing photography equipment. Although phone camera technology has improved in recent years, there may be advantages to using photography equipment and improved photo quality may increase the proportion of +Ms (Bendik et al. 2013; Nipko et al. 2020).

The efficacy of using photographs for animal identification relies on the sample size. The efficacy of HotSpotter relies on collecting a large set of photos of similar quality for the total population and for each individual. HotSpotter software has been implemented into the citizen science platform, Wildbook (Berger-Wolf et al. 2017), which is a collection of shared, autonomous databases. Each database contains images collected by a variety of individuals that aid in both species and individual identification. There are currently several Wildbooks for different animals including whales (Flukebook; http://flukebook.org), whale sharks (http://whaleshark.org), Saimaa ringed seals (http://norppagalleria .wwf.fi), lynx (http://lynx .wildbook.org), and sea turtles (Internet of Turtles; http://iot .wildbook.org/). We suggest that a Wildbook dedicated to bats could help create an easily accessible and rich database for all bat biologists, help in conservation and management programs, and/or possibly be used as a tool for determining bat species (Cheney et al. 2017).

Although HotSpotter appears to be effective identifying bats, there are other FBPs that may be used including I3S Pattern+ (Van Tienhoven et al. 2007) and Wild-ID (Bolger et al. 2012). Wild-ID and HotSpotter both implement the SIFT algorithm for feature detection and comparisons; however, Wild-ID does

not implement an LNNBNN algorithm to perform one-versus-many comparisons. Researchers may also be inclined to use PBPs (e.g. Matthé et al 2017; Moya et al 2015) as they tend to have better accuracy compared to FBPs. However, PBPs are very sensitive to changes in image quality, resolution, size, and orientation. Thus, using a shared photo database (e.g. Wildbook) may not be feasible unless similar equipment and standardized photo collection were employed. For these reasons, we believe HotSpotter is best suited to detect and compare CE patterns in bats.

The use of wing membrane photographs to evaluate ecological / conservational questions may introduce some barriers. Researchers collecting photos may be subject to observer biases (Marsh and Hanlon, 2007) from sampling at certain locations more regularly than others, or at certain times of the year where bats are abundantly caught. Seasonal factors may also affect data collection as dry / splotchy wing membrane (usually seen in colder climates) may reduce the visibility of CE bundle patterns. Moreover, data collection may be limited during torpor periods to reduce animal stress (Barclay and Bell, 1988). Different practices in photo collection between researchers including camera models and settings may make it difficult to accurately compare across datasets. Thus, introducing a bat-specific Wildbook may be accompanied by hesitations, considering that it is an open access database. Researchers need to consider the benefits and challenges that are attributed to having an open access database of collected photos (e.g. Dickinson et al. 2010; van Strien et al. 2013).

Effective Biomarker – Altogether, CE bundles appear to be an effective biomarker as they are universal, distinct, collectable and permanent (Amelon et al.

2017; Jain et al. 2004). Despite variability between bats, every bat we photographed had CE bundles that were visible in the photos. As for permanence, we did not notice any changes in wing morphology or CE bundle patterns during the study. Ideally, we would record over a longer duration to get a better understanding of CE bundle pattern permanence.

Our results suggest that HotSpotter has the potential to accurately and reliably identify big brown bats (*Eptesicus fuscus*) based on the pattern of CE bundles in their wing membranes. We used the default settings in HotSpotter, but by adjusting these settings to change the sensitivity of feature detection within chips and/or allow users to accept/reject certain feature comparisons between photos (e.g. when two features being compared across the *qcid* and *cid* are clearly of different portions of the wing membrane), users may be able to increase the efficacy of HotSpotter. Future studies should examine if HotSpotter is able to identify and distinguish individuals of other bat species or accurately discriminate bat species. Although we believe HotSpotter can accurately detect individual bats based on the unique CE bundle patterns in their wing membranes, we advise testing this technique in the field in conjunction with another marking technique (e.g. banding) to get a better understanding of its applicability.

Literature Cited – Chapter 3: Using HotSpotter to identify individual big brown bats (*Eptesicus fuscus*) via collagen-elastin bundle patterns

Agresti A., Coull B. A. 1998. Approximate is better than "exact" for interval estimation of binomial populations. The American Statistician 52:119–126.

Amelon S. K., Hooper S. E., Womack K. M. 2017. Bat wing biometrics: using collagen-elastin bundles in at wings as a unique individual identifier. Journal of Mammalogy 98:744–751.

Baldi B., and Moore D. S. 2014. The practice of statistics in the life sciences. Third edition. W. H. Freeman and Company, New York, New York, USA.

Barclay R. M. R., Bell G. P. 1988. Marking and observational techniques. In: Kunz T.H., editor. Ecological and behavioural methods for the study of bats. Smithsonian Institution Press; p. 59–76.

Bendik N. F., Morrision A., Gluesenkamp A. G., Sanders M. S. O'Donnell L. J. 2013. Computer-assisted photo identification outperforms visible implant elastomers in an endangered salamander, *Eurycea tonkawae*. PLoS One 8:e59424.

Berger-Wolf T. Y., Crall J. P., Holberg J., Parham J., Stewart C., Mackey B. L., Kahumbu P., Rubenstein D. 2016. The great Grevy's rally: the need, methods, findings, implications and next steps. Grevy's Zebra Trust, Nairobi, Kenya, Tech. Rep.

Berger-Wolf T. Y., Rubenstein D. I., Stewart C. V., Holmberg J. A., Parham J., Menon S., Crall J. P., Van Oast J., Kiciman E., Joppa L. 2017. Wildbook: Crowdsourcing computer vision, and data science for conservation. arXiv preprint arXiv:1710.08880.

Blount D., Bohnett E., Holmberg J., Parham J., Faryabi S. P., Johansson O., An L., Ahmad B., Khan W., Ostrowski S. 2022. Comparison of two individual identification algorithms for snow leopards after automated detection. BioRxiv.

Bohnett E., Poya F. S., Lewison R., An L., Bian X., Rajabi A. M., Jahed N., Rooyesh H., Mills E., Ramos S., Mesnildrey N., Santoro P. C. M., Taylor J., Terentyev V., Ostrowski S. 2023. Human expertise combined with artificial intelligence improves performance of snow leopard camera trap studies. Global Ecology and Conservation 41:e02350.

Bolger D. T., Morrison T. A., Vance B., Lee D., Farid H. 2012. A computer-assisted system for photographic mark-recapture analysis. Methods in Ecology and Evolution 3:813–822.

Brewer C. T., Rauch-Davis W. A., Fraser E. E. 2021. The use of intrinsic markers for studying the migratory movements of bats. Animals 11:3477.

Brtizke E. R., Duchamp J. E., Murray K. L., Swihart, R. K., Robbins L. W. 2011. Acoustic identification of bats in the eastern United States: A comparison of parametric and nonparametric methods. The Journal of Wildlife Management 75:660–667.

Buchlear E. R. 1980. The development of flight, foraging, and echolocation in the little brown bat (*Myotis lucifugus*). Behavioural Ecology and Sociobiology 6:211–218.

Burgstaller S., Gollmann G., Landler L. 2021. The green toad example: A comparison of pattern recognition software. North-West Journal of Zoology 17:96–99.

Ceballos-Vasquez A., Caldwell J. R., Faure P. A. 2014a. A device for restraining bats. Acta Chiropterologica 16:255–260.

Ceballos-Vasquez A., Caldwell J. R., Faure P. A. 2014b. Seasonal and reproductive effects on wound healing in the flight membranes of captive big brown bats. Biology Open 4:95–103.

Cheema G. S., Anand S., Altun Y., Das K., Mielikäinen T., Malerba D., Stefanowski J., Read J., Žitnik M., Ceci M., Džeroski S. 2017. Automatic detection and recognition of individuals in patterned species. Machine Learning and Knowledge Discovery in Databases 27–38.

Cheeseman T., Southerland K., Park J., Olio M., Flynn K., Calambokidis J., Jones L., Garrigue C., Frisch J. A., Howard A., Reade W., Neilson J., Gabriele C., Clapham P. 2022. Advanced image recognition: a fully automated, high-accuracy photo-identification matching system for humpback whales. Mammalian Biology 102:915–929.

Cheney J. A., Allen J. J., Swartz S. M. 2017. Diversity in the organization of elastin bundles and intramembranous muscles in bat wings. Journal of Anatomy 230:510–523.

Cheney J. A., Konow N., Bearnot A., Swartz S. M. 2015. A wrinkle in flight: the role of elastin fibres in the mechanical behaviour of bat wing membranes. Journal of the Royal Society Interface 12:20141286.

Christian J. J. 1956. The natural history of a summer aggregation of the big brown bat, *Eptesicus fuscus.* American Midland Naturalist 66–95.

Church J. C. T., Warren D. J. 1968. Wound healing in the web membrane of the fruit bat. British Journal of Surgery 55:26–31.

Crall J. P., Stewart C. V., Berger-Wolf T. Y., Rubenstein D. I., Sundaresan S. R. 2013. HotSpotter – Patterned species instance recognition. 2013 IEE Workshop on Applications of Computer Vision (WACV). 230–237.

Dickinson J. L., Zuckerberg B., Bonter D. N. 2010. Citizen science as an ecological research tool: challenges and benefits. Annual Review of Ecology, Evolution, and Systematics 41:149–172.

Duhé S. 2018. Using HotSpotter animal individual recognition software in the detection of ontogenetic pattern changes in Panamanian golden frogs (*Atelopus zeteki*) [undergraduate thesis]. [Mechanicsburg (PA, USA)]: Messiah University.

Dunbar S. G., Anger E. C., Parham J. R., Kingen C., Wright M. K. 2021. HotSpotter: Using a computer-driven photo-id application to identify sea turtles. Journal of Experimental Marine Biology and Ecology, 535:151490.

Faure P. A., Re D. E., Clare E. L. 2009. Wound healing in the flight membranes of big brown bats. Journal of Mammalogy 90:1148–1156.

Gaston K. J., O'Neill M. A. 2004. Automated species identification: why not?. Philosophical Transactions of the Royal Society of London. Series B: Biological Sciences 359:655–667.

Gosline J., Lilllie M., Carrington E., Guerette P., Ortlepp C., Savage K. 2002. Elastic proteins: biological roles and mechanical properties. Philosophical Transactions of the Royal Society of London, B. Biological Sciences 357:121–132.

Greville L. J., Ceballos-Vasquez A., Valdizon-Rodriguez R., Caldwell J. R., Faure P. A. 2018. Wound healing in wing membranes of the Egyptian fruit bat (*Rousettus aegyptiacus*) and big brown bat (*Eptesicus fuscus*). Journal of Mammalogy 99:974–982.

Guo S. A., DiPietro L. A. 2010. Factors affecting wound healing. Journal of Dental Research 89:219–229.

Hanna M. E., Chandler E. M., Semmens B. X., Eguchi T., Lemons G. E., Seminoff J. A. 2021. Citizen-sourced sightings and underwater

photography reveal novel insights about green sea turtle distribution and ecology in Southern California. Frontiers in Marine Science 8:671061.

Harmsen B. J., Saville N., Foster R. J. 2021. Long-term monitoring of margays (*Leopardus wiedii*): Implications for understanding low detection rates. PLOS ONE 16:e0247536.

Hodgkison R., Balding S. T., Akbar Z., Kunz T. H. 2003. Roosting ecology and social organization of the spotted-winged fruit bat *Balionycteris malculata* (Chiroptera: Pteropodidae), in a Malaysian lowland dipterocarp forest. Journal of Tropical Ecology 19:667–676.

Holbrook K. A., Odland G. F. 1978. A collagen and elastic network in the wing of the bat. Journal of Anatomy 126:21–36.

Hood W. R., Bloss J., Kunz T. H. 2002. Intrinsic and extrinsic sources of variation in size at birth and rates of postnatal growth in the big brown bat, *Eptesicus fuscus* (Chiroptera: Vespertilionidae). Journal of Zoology 258:355–363.

Jain A. K., Ross A., Prabhakar S. 2004. An introduction to biometric recognition. IEEE Transactions on Circuits and Systems for Video Technology 14:4-20.

Khan C., Blount D., Parham J., Holmberg J., Hamilton P., Charlton C., Chritiansen F., Johnston D., Rayment W., Dawson S., Vermeulen E., Rowntree V., Groch K., Levenson J. J., Bogucki R. 2022. Artificial

intelligence for right whale photo identification: from data science competition to worldwide collaboration. Mammalian Biology 102:102–1042.

Kurta A., Baker R. H. 1990. *Eptesicus fuscus*. Mammalian Species 356:1–10.

Kurta A., Rogers C., Gmutza H. J., Wilson A. K., Schaetz B. A., Munzer O. M., ... Kurta M. (2023). Ultraviolet light reveals cryptic markings in Greater Antillean Long-tongued bats (*Monophyllus redmani*) from Puerto Rico. Journal of North American Bat Research 1(1).

Lea J. M. D., Walker S. L., Kerley G. I. H., Jackson J., Matevich S. C., Shultz, S. 2018. Non-invasive physiological markers demonstrate link between habitat quality, adult sex ratio and poor population growth rate in vulnerable species, the Cape mountain zebra. Functional Ecology 32:300–312.

Lemon J. 2006. Plotrix: a package in the red light district of R. R-News 6:8–12.

Lollar A., Schmidt-French B. 1998. Captive care and medical reference for the rehabilitation of insectivorous bats. Bat World Publications, Mineral Wells, Texas.

Lowe D. G. 2004. Distinctive image features from scale-invariant keypoints. International Journal of Computer Vision 60:91–110.

Marsh D. M., Hanlon T J. 2007. Seeing what we want to see: Confirmation bias in animal behaviour research. Ethology 113:1089–1098.

Matthé M. M., Sannolo M., Winiarski K., Spizen-van der Sluijs, Goedbloed D., Steinfartz S., Stachow U. 2017. Comparison of photo-matching algorithms commonly used for photographic capture-recapture studies. Ecology and Evolution 7:5861–5872.

Mayberry H. W., Faure P. A. 2014. Morphological, olfactory, and vocal development in big brown bats. Biology Open 4:22–34.

McCann S., Lowe D. G. 2012. Local Naïve Bayes Nearest Neighbour for image classification. 2012 IEEE Conference on Computer Vision and Pattern Recognition, 3650–3656.

Miguel A., Bayrakçismith R. Ferre E., Bales-Heisterk C., Beard J., Dioso M., Grob D., Hartley R., Nguyen T., Weller N. 2019. Identifying individual snow leopards from camera trap images. Tenth International Conference on Signal Processing Systems 11071:138–142.

Mikolajczyk K., Tuytelaars T., Schmid C., Zisserman A., Matas J., Schaffalitzky F., Kadir T., Gool L. 2005. A comparison of affine region detectors. International Journal of Computer Vision 65:43–72.

Moss C. F., Redish D., Gounden C., Kunz T. H. 1997. Ontogeny of vocal signals in the little brown bat, *Myotis lucifugus*. Animal Behaviour 54:131–141.

Moya O., Mansilla P. L., Madrazo S., Igual J. M., Rotger A., Romano A., Tavecchia G. 2015. APHIS: a new software for photo-matching in ecological studies. Ecological Informatics 27:64–70.

Murray K. L., Britzke E. R., Robbins L. W. 2001. Variation in search-phase calls of bats. Journal of Mammalogy 82:728–737.

Nepovinnykh E., Vilkman A., Eerola T., Kälviäinen H., Gade R., Felsberg M, Kämäräinen, J-K. 2023. Re-identification of Saimaa ringed seals from image sequences. In *Scandinavian Conference on Image Analysis* 111–125. Cham: Springer Nature Switzerland.

Nipko R. B., Holcombe B. E., Kell M. J. 2020. Identifying individual jaguars and ocelots via pattern-recognition software: Comparing HotSpotter and Wild-ID. Wildlife Society Bulletin 44:424–433.

O'Farrell M. J., Gannon W. L. 1999. A comparison of acoustic versus capture techniques for the inventory of bats. Journal of Mammalogy 80:24–30.

O'Farrell M. J., Studier E. H. 1973. Reproduction, growth, and development in *Myotis thysanodes* and *M. lucifugus* (Chiroptera: Vespertilionidae). Ecology 54:18–30.

Olsen E. O. 2023. Scanner imaging of common sharp-tailed snakes (*contia tenuis*) for individual identification. Northwestern Naturalist 104:26–36.

Park H., Lim A., Choi T-Y., Baek S-Y., Song E-G., Park Y. C. 2019. Where to spot: individual identification of leopard cats (*Prinailurus bengalensis euptilurus*) in South Korea. Journal of Ecology and Environment. 43:39.

Patel N. G., Das A. 2020. Shot the spots: A reliable field method for individua identification of Amolop formosus (*Anura Ranidae*). Herpetozoa 33:7–15.

Perd'och M., Chum O., Matas J. 2009. Efficient representation of local geometry for large scale object retrieval. In 2009 IEEE Conference on Computer Vision and Pattern Recognition (pp. 9–16). IEEE.

Quinby B. M., Creighton J. C., Flaherty E. A. 2021. Estimating population abundance of burying beetles using photo-identification and mark-recapture methods. Environmental Entomology 50:238–246.

Satterthwaite F. E. 1946. An approximate distribution of estimates of variance components. Biometrics bulletin 2:110–114.

Smyth L. K., Balme G. A., Tyzack-Pitman R., Bishop J. M., O'Riain J. M. 2022. Like mother like daughter: quantifying the relationship between relatedness and phenotypic similarity in leopard pelage patterns. Mammalian Biology 1–16.

Swartz S. M., Allen J. J. 2020. Structure and function of bat wings: A view from the Phyllostomidae. In TH Fleming, LM Dávalos, and MAR Mello, eds., Phyllostomid Bats: A Unique Mammalian Radiation, 151–168. Chicago: University of Chicago Press.

Tabuki K., Nishizawa H., Abe O., Okuyama J., Tanizaki S. 2021. Utility of carapace images for long-term photographic identification of nesting green turtles. Journal of Experimental Marine Biology and Ecology 545:151632.

Timpe A., Zhang S., Hubner J., Ukeiley L. 2013. Passive flow control by membrane wings for aerodynamic benefit. Experiments in Fluids 54:1–23.

Van Strien A. J., van Swaay C. A., Termaat T. 2013. Opportunistic citizen science data of animal species produce reliable estimates of distribution trends if analysed with occupancy models. Journal of Applied Ecology 50:1450–1458.

Van Tienhoven A. M., Den Hartog J. E., Reijns R. A. Peddemors V. M. 2007. A computer-aided program for pattern matching of natural marks on the spotted reggedtooth shark *Carcharias taurus.* Journal of Applied Ecology 44:273–280.

Vaughan T. A. 1970. Adaptions for flight in bats. In *About Bats, A Chiropteran Symposium* (ed. B. H. Slaughter & D. W. Walton), pp.127–143. Dallas: Southern Methodist University Press.

Vilkman A. 2022. One-to-many and many-to-many matching for Saimaa ringed seal re-identification [master's thesis]. [Lappeenranta, Finland]: Lappeenranta-Lahti University of Technology

Wickham H., Chang W., Wickham M. H. Package 'ggplot2'. Create elegant data visualizations using the grammar of graphics. Version 2:1–189.

Chapter 4 – Conclusion

Conclusion

Our studies suggest that both p-Chip and HotSpotter methods are viable in distinguishing individual big brown bats (*Eptesicus fuscus*). These methods address some of the caveats attributed to commonly used marking methods in bats. Owing to their relatively small size (500 × 500 μm), p-Chips are a reasonable alternative to commonly used PIT tags as p-Chips are considerably less invasive. Alternatively, HotSpotter has the major benefit of taking away the need to apply external tags to bats. Although animal handling is required to collect images of bat wing membrane, researchers do not have to add anything to or manipulate the animals appearance to consider an animal *marked*.

No marking method is superior to all others. This includes p-Chips and HotSpotter as each present caveats of their own. For instance, the size of the p-Chip tag and the wands read range make animal handling a necessity to visualize and properly scan tagged bats. Similar to other external markers (e.g. bands), the location of p-Chip implantation must be standardized within the community of bat researchers for effective use. HotSpotter introduces the caveat of possible misidentification, as the software provides the most probable match and relies on visual inspection for confirmation. Table 4.1 compares various tag characteristics between p-Chip and HotSpotter use in big brown bats (*Eptesicus fuscus).*

Typically, marking methods are chosen to compliment the experiment being conducted. For example, PIT tags are more suitable for conducting passive readings for individual bats compared to plastic split-ring bands because PIT tags

can be scanned without animal handling. Using p-Chips and/or HotSpotter may be more adept in certain situations compared to alternative marking methods for some situations. For example, p-Chips may be suitable for use in captive bat colonies or for museum specimens where regular handling may be more common, but may be unsuitable for situations where recapture rates are less common. HotSpotter may be beneficial for use where recapture rates are high and there are abundant opportunities to take photos of individuals and populations of bats.

Selecting a marking method can also depend on the species being studied. For example, some species of bats may be too small to have tags injected subcutaneously (e.g. PIT tags) or tags of significant weight applied (Barclay & Bell, 1988), some may be intolerant / less tolerant to certain marking methods (Hodgkison et al. 2003; Bradbury 1977), may be more likely to chew on external tags, or more likely to incur injury as a result of either the tagging and/or scanning procedures. In our studies, we used big brown bats (*Eptesicus fuscus*) from a captive colony at McMaster University. Our studies suggest that using p-Chip tags and/or HotSpotter to evaluate collagen-elastin bundles may be suitable to mark *E. fuscus*, but do not address the efficacy of these methods in other bat species. For the many marking techniques currently available, there are limited guidelines on marking method selection (Barnard, 1988; Kunz 1996; Lollar and Schmidt-French 1998; Powell and Proulx, 2003; Kunz & Weise 2009).

Overall, the purpose of this thesis was to introduce two new alternatives for marking individual bats. Both methods appear to be viable for use in big brown bats (*Eptesicus fuscus*). We recommend that both p-Chip and HotSpotter

methods be tested in free-ranging bat populations, and in different bat species to gain a better appreciation of their efficacy. The introduction of p-Chips and HotSpotter is not meant to replace pre-existing methods, but to provide viable marking alternatives that address the caveats associated with commonly used marking methods.

Table. 4.1.—Features of p-Chips, and collagen-elastin for marking bats.

Information is based on data from this MSc Thesis.

Tag Characteristic	p-Chips	Collagen-Elastin
Composition	semi-conductor	biometric marker
Invasive Application?	yes (subcutaneous)	no
USDA/CCAC Rating	Category C	N/A
Pain/Duration	minor/short	minor/short
Application Tool?	sterile needle (21 G)	none
Application Injury?	yes (bleeding); possible limb or tendon damage, infection	none
Post-Application	possible inflammation,	N/A
Morbidity / Mortality	infection / not reported	not reported (unlikely)
Affects Behaviour?	not reported	not reported (unlikely)
Location	no standard location	wing membrane
Code	digital RFID 9-didgit (alphanumeric code)	none
Size	500 × 500 × 100 µm (l × w × h)	depends on wing size
Bat Size Restriction?	not tested (likely none)	not tested (likely none)
Bat Handling Required?	yes	yes
Removable?	no (requires surgery)	no (intrinsic to wing)
Reusable?	not tested; (requires sterilization)	yes
Reader	laser wand connected to computer	Camera[§]
Reader Range	≤10 mm chip surface with photocell	not tested (depends on camera)
Reader Orientation	p-Chip surface with photocell	ventral surface of wing
Visible?	yes (varies with skin pigmentation)	yes
Persistence	lifetime (but tag can flip and be obscured *in situ*)	lifetime†
Tag Loss?	possible (unseen in wing)	no (unless wing is sufficiently damaged)
Readability	100% success in wing and variable success in leg	60% success in adult database, 27 % success in juvenile database
Training Required?	minimal (for subcutaneous injection)	minimal (HotSpotter User Guide)
Tag Cost	$2.00 USD	N/A
Reader Cost	$2000 USD	Variable based on camera
Detection Software	p-Chip Corp. Software	HotSpotter (Crall et al. 2013)
Software Availability	p-Chip Corp.	free-to-use
Compatibility	internally compatible	Mac, Windows, Linux
Field Tested?	no	no

*results of present study suggest 2nd metacarpal as a prospective location for small-to-medium-sized bats

[§]Quality likely varies with different camera models being used. iPhone 11 used in this study

†Currently unknown when collagen-elastin bundles fully develop or whether they change in response to wing injury

References – Introduction (Chapter 1) and Conclusion (Chapter 4)

Aldridge H. D. J. N., Brigham R. M. 1988. Load carrying and maneuverability in an insectivorous bat: a test of the 5% "rule" of radio-telemetry. Journal of mammalogy 69:379–382.

Baker G. B., Lumsden L. F. Dettmann E. B., Schedvin N. K., Schulz M., Watkins D., Jansen L. 2001. The effect of forearm bands on insectivorous bats (Microchiroptera) in Australia. Wildlife Research 28:229–237.

Barnard S. M. 1989. The use of microchip implants for identifying big brown bats (*Eptesicus fuscus*). Animal Keepers Forum 16:50–52.

Barnard S. M. Abram D. 2004. Body piercing as a method of marking captive bats. Research News 45:11–15.

Barbour, R. W., & Davis, W. H. 1969. Bats of America. University Press Kentucky, Lexington, 286 pp.

Barclay R. M. R., Bell G. P. 1988. Marking and observational techniques. In: Kunz T.H., editor. Ecological and Behavioural Methods for the Study of Bats. Smithsonian Institution Press; p. 59–76.

Bonaccorso F. J., Smythe N. 1972. Punch-marking bats: an alternative to banding. Journal of Mammalogy 53:389–390.

Bonaccorso F. J., Smythe N., Humphrey S. R. 1976. Improved techniques for marking bats. Journal of Mammalogy 57:181–182.

Brack V., Twente J. 2011. The duration of the period of hibernation of three species of vespertilionid bats. I. Field Studies. Canadian Journal of Zoology 63:2952–2954.

Bradbury J. W. 1977. Lek mating behaviour in the hammer-headed bat. Zeitschrift für Tierpsychologie 45:225–255.

Britzke E. R., Gumbert M. W. Hohmann M. G. 2014. Behavioural response of bats to passive integrated transponder tag reader arrays placed at cave entrances. Journal of Fish and Wildlife Management 5:146–150.

Brooke A. P. 1987. Tent selection, roosting ecology and social organization of the tent-making bat, *Ectophylla*, in Costa Rica. Journal of Tropical Ecology 3:171–175.

Buchlear E. R. 1976. A chemiluminescent tag for tracking bats and other small nocturnal animals. Journal of Mammalogy 57:173–176.

Caccamise D. F. Heddin R. S. 1985. An aerodynamic basis for selecting transmitter loads in birds. The Wilson Bulletin 306–318.

Gannon M. R. 1994. A new technique for marking bats. Bat Research News 34:88–89.

Gifford C. E., Griffin D. R. 1960. Notes on homing and migratory behaviour of bats. Ecology 41:378–381.

Griffin D. R. 1934. Marking bats. Journal of Mammalogy 15:202–207.

Handley Jr. C. O., Wilson D. E., Gardner A . L. 1991. Methods of capturing and marking tropical bats. Demography and Natural History of the Common Fruit Bat.

Happold D., Happold M. 1997. Effects of bat-bands and banding on a population of *Pipistrellus nanus* (Chiroptera: Vespertilonidae) in Malawi. Zeitschrift für Saugetierkunde 63:65–78.

Herried C. F., Davis R. B., Short H. L. 1960. Injuries due to bat banding. Journal of Mammalogy 41:398–400.

Hitchcock H. B. 1957. The use of bird bands on bats. Journal of Mammalogy 38:402–405.

Hodgkison R., Balding S. T., Akbar Z., Kunz T. H. 2003. Roosting ecology and social organization of the spotted-winged fruit bat *Balionycteris malculata* (Chiroptera: Pteropodidae), in a Malaysian lowland dipterocarp forest. Journal of Tropical Ecology 19:667–676.

Hovorka M. D., Marks C. S., Muller E. 1996. An improved chemiluminescent tag for bats. Wildlife Society Bulletin 24:709–712.

Kunz T. H. 1996. Methods of marking bats. In: Wilson D. E., Cole F. R., Nichols J. D., Rudran R., Foster M. S., editors. Measuring and Monitoring Biological Diversity: Standard Methods for Mammals. Smithsonian Institution Press; p. 304–310.

Kunz T. H., Weise C. D. 2009. Methods and devices for marking bats. In: Kunz T.H., Parsons S., editors. Ecological and Behavioural Methods for the Study of Bats. 2nd Edition. The John Hopkins University Press; p. 36–56.

LaVal R. K., Clawson R. L., LaVal M. L., Caire W. 1977. Foraging behaviour and nocturnal activity patterns of Missouri bats, with emphasis on the

endangered species *Myotis grisesens* and *Myotis sodalis.* Journal of Mammalogy 58:592–599.

Lazarus A. B., Rowe F. P. 1975. Freeze-marking rodents with a pressurized refrigerant. Mammal Review 5:31–34.

Leblanc D. M., Reeder D. M., Kosreczko N. S. 2002. Individual marking of captive flying foxes for behavioural observations. Bat Research News 43:163.

LeMunyan C. D., White W., Nyberg E., Christian J. J. 1959. Design of a miniature radio transmitter for use in animal studies. The Journal of Wildlife Management 23:107–110.

Lollar A., Schmidt-French B. 1998. Captive care and medical reference for the rehabilitation of insectivorous bats. Bat World Publications, Mineral Wells, Texas.

Mohr C. E. 1934. Marking bats for later recognition. Proceedings of the Pennsylvania Academy of Science 8:26–30.

Norman A. P., Jones G., Arlettaz R. 1999. Noctuid moths show neural and behavioural responses to sounds made by some bat marking rings. Animal Behaviour 57:829–835.

Phillips W. R. 1985. The use of bird bands for marking tree-dwelling bats as a preliminary appraisal. Macroderma 1:17–21.

Pierson E. D., Fellers G. M. 1994. Injuries to *Piecotus townsendii* from lipped wing bands. Bat Research News, 34:89–91.

Powell R. A., Proulx G. 2003. Trapping and marking terrestrial mammals for research: integrating ethics, performance criteria, techniques, and common sense. Institute for Laboratory Animal Research 44:259–276.

Punt A. 1957. The use of radioactive bands in tracing hibernating bats. Experientia. 13:51–54.

Sherwin R. E., Haymond S., Stricklan D., Oslen R. 2002. Freeze-branding to permanently mark bats. Wildlife Society Bulletin 30:97–100.

Silvy N. J., Lopez R. R., Peterson M. J. 2012. Techniques for marking wildlife. The Wildlife Techniques Manual: Research (7th Ed., pp 230-257). Baltimore MD: John Hopkins University Press.

Speakman J. R., Thomas D. W., Kunz T. H., Fenton M. B. (2003). Physiological ecology and energetics of bats. Bat ecology, 430–490.

Stebbings R. E. 1978. Marking bats. In: Mitchell-Jones A. J., McLeish A. P., editors. The Bat Workers' Manual. Nature Conservancy Council, Interpretive Services Branch; p. 52–62.

Stebbings R. E. 2004. Ringing and marking. Bat Workers Manual 59–62.

Tidemann C. R. 2002. Sustainable management of the grey-headed flying-fox *Pteropus poliocephalus*. Managing the Grey-headed Flying-fox as a Threatened Species in NSW, 122–127.

Trapido H., Crowe P. E. 1946. A wing-banding method in the study of the travel of bats. Journal of Mammalogy 27:224–226.